CBCS SCHEME

USN | | | | | | | | | | |

BEC703

Seventh Semester B.E./B.Tech. Degree Examination, Dec.2025/Jan.2026
Wireless Communication Systems

Time: 3 hrs. Max. Marks: 100

Note: 1. Answer any FIVE full questions, choosing ONE full question from each module.
2. M : Marks , L: Bloom's level , C: Course outcomes.

		Module – 1	M	L	C
Q.1	a.	Derive an Expression for Rayleigh Fading Wireless Channel.	10	L2	CO2
	b.	In the wireless Rayleigh fading channel consider a transmit power Pt (dB) = 20 dB. What is the probability that the power at the receiver is greater than Pr(dB) = 10 dB?	10	L2	CO1
		OR			
Q.2	a.	Explain the modeling of wireless systems with proper equations.	10	L2	CO1
	b.	Give the mathematical equations for RMS Delay Based on Average Power Profile.	10	L2	CO1
		Module – 2			
Q.3	a.	Explain the Properties of PN sequences.	10	L2	CO1
	b.	Explain any two advantages of CDMA.	10	L2	CO1
		OR			
Q.4	a.	Illustrate OFDM with an example.	10	L2	CO1
	b.	With neat schematic explain MIMO-OFDM Transmitter.	10	L2	CO1
		Module – 3			
Q.5	a.	Explain GSM Network Architecture.	10	L2	CO1
	b.	Explain IP-Based Flat Network Architecture.	10	L2	CO1
		OR			
Q.6	a.	Explain Multi Antenna techniques.	10	L2	CO1
	b.	Explain LTE Network Architecture with necessary diagram.	10	L2	CO1
		Module – 4			
Q.7	a.	Explain MIMO System Model.	10	L2	CO1
	b.	Derive Expression for MIMO Zero-Forcing (ZF) Receiver.	10	L2	CO1

		OR			
Q.8	a.	Compute the MIMO zero-forcing receiver for the channel matrix H given $H = \begin{bmatrix} 2 & 3 \\ 1 & 3 \\ 1 & 2 \end{bmatrix}$	10	L3	CO2
	b.	Derive expression for MIMO MMSE Receiver.	10	L2	CO1
		Module – 5			
Q.9	a.	With neat diagram, explain design principles of LTE Network.	10	L2	CO1
	b.	Explain the Hierarchical Channel Structure of LTE.	10	L2	CO1
		OR			
Q.10	a.	Explain the time domain frame structures of OFDM.	10	L2	CO1
	b.	Explain Uplink SC-FDMA Radio Resources.	10	L2	CO1

* * * * *

Qn 1a

The complex fading coefficient h can be expressed in terms of its real and imaginary components as,

$$h = ae^{j\phi} = \sum_{i=0}^{L-1} (x_i + jy_i) = X + jY$$

Thus, X, Y, which are the real and imaginary components of the fading coefficient $ae^{j\phi}$, are derived from the summation of a large number of random multipath components x_i, y_i, especially in a rich urban setting which allows for a large number of scatterers. Hence, it is reasonable to assume that X, Y are random in nature. Further, a simplistic model for the statistical characterization of X, Y would be to assume that they are *Gaussian* and un-correlated. The assumption of Gaussianity is lent support by the *central limit theorem*, which in simple terms states that a normalized random variable derived from the sum of a large number of independent identically distributed random components, converges to a Gaussian random variable.

The above assumption is valid as $L \to \infty$, i.e., the number of multipath components is fairly large. Hence, X, Y are distributed as $\mathcal{N}\left(0, \frac{1}{2}\right)$ (assuming zero-mean and variance $\frac{1}{2}$). Further, since X, Y are Gaussian in nature and un-correlated, it directly follows that they are *independent*. The joint distribution of X, Y is given by the standard multivariate Gaussian as

$$f_{X,Y}(x, y) = \frac{1}{\pi} e^{-(x^2+y^2)}$$

One can now derive the statistics of the fading coefficient $ae^{j\phi}$ in terms of its amplitude and phase factors a, ϕ. It can be seen through elementary trigonometric properties that

$$x = a\cos\phi, \;\; y = a\sin\phi$$

The joint distribution $f_{A,\Phi}(a, \phi)$ can be derived from $f_{X,Y}(x, y)$ using the relation for multivariate PDF transformation as

$$f_{A,\Phi}(a, \phi) = \frac{1}{\pi} e^{-a^2} J_{X,Y}$$

where we have used the property that $x^2 + y^2 = a^2$ in the above expression. The quantity $J_{X,Y}$ is termed the Jacobian of X, Y and is given by the expression

$$J_{X,Y} = \left| \begin{bmatrix} \cos\phi & \sin\phi \\ -a\sin\phi & a\cos\phi \end{bmatrix} \right| = a$$

where $|\mathbf{A}|$ denotes the determinant of the matrix $\mathbf{A}$. Substituting the Jacobian in the expression for multivariate PDF transformation above, the joint PDF with respect to the random variables A, Φ can be derived as

$$f_{A,\Phi}(a,\phi) = \frac{a}{\pi} e^{-a^2}$$

The marginal distributions f_A, f_Φ with respect to the amplitude and phase factor random variables A, Φ can be readily derived from the above joint distribution as

$$f_A(a) = \int_{-\pi}^{\pi} f_{A,\Phi}(a,\phi)\, d\phi = 2ae^{-a^2}, 0 \leq a \leq \infty$$

$$f_\Phi(\phi) = \int_0^{\infty} f_{A,\Phi}(a,\phi)\, da = \frac{1}{2\pi} e^{-a^2}\Big|_0^{\infty} = \frac{1}{2\pi}, -\pi < \phi \leq \pi$$

We have now derived one of the most popular and frequently employed models for the wireless channel, termed a *Rayleigh fading* wireless channel. This nomenclature arises from the distribution f_A of the amplitude factor a, which is the well known Rayleigh density, shown in Figure 3.3. Observe that the average power in the amplitude a of the Ralyeigh fading channel coefficient h is given as

$$\mathrm{E}\left\{|h|^2\right\} = \mathrm{E}\left\{a^2\right\} = \mathrm{E}\left\{X^2 + Y^2\right\} = 1$$

Further, it is important to note that although strictly speaking, the term Rayleigh refers to the distribution of the amplitude factor, the Rayleigh fading wireless channel characterizes both

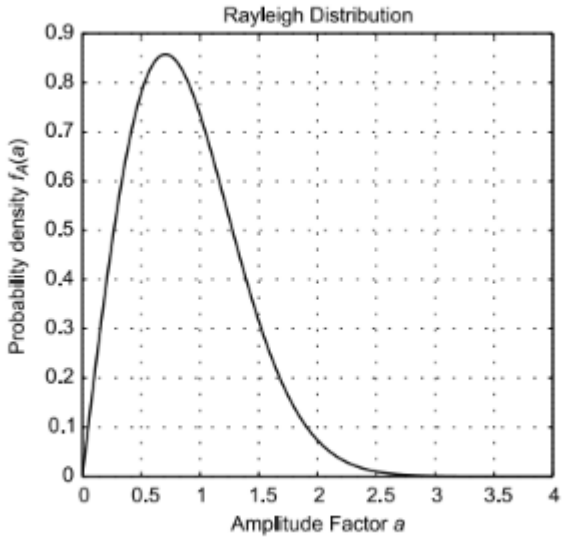

Figure 3.3 *Rayleigh density for amplitude factor a*

the amplitude factor as a Rayleigh fading random variable and the phase factor as uniformly distributed in $(-\pi, \pi)$. Finally, it can be readily seen that the joint distribution $f_{A,\Phi}(a,\phi)$ is related to the marginals $f_A(a), f_\Phi(\phi)$ as,

$$f_{A,\Phi}(a,\phi) = f_A(a)\, f_\Phi(\phi)$$

essentially implying that the random variables A, Φ are *independent*. This is a fairly important result since it suggests that the random varying nature of the phase factor of the arriving signal is independent of that of the amplitude, i.e., for a given amplitude a, all phase factors in $(-\pi, \pi)$ are equiprobable. Figure 3.4 shows a scatter plot of the real and imaginary components of 10000 randomly generated samples of the Rayleigh fading coefficient. From the circular symmetry of the plot, it can be readily seen that the phase of the Rayleigh coefficient is distributed uniformly in $(-\pi, \pi)$.

Qn 1 b

In the wireless Rayleigh fading channel described above, consider a transmit power $P_t\,(\text{ dB}) = 20$ dB. What is the probability that the power at the receiver is greater than $P_r\,(\text{ dB}) = 10$ dB ?

Solution: First, let us begin by computing the appropriate linear power values for the above given dB values. $P_t\,(\text{ dB}) = 10\log_{10}(P_t)$. Hence, the linear transmit power P_t is given as $P_t = 10^{P_t(\text{ dB})/10} = 10^2 = 100$. Similarly, the linear receiver power corresponding to $P_r\,(\text{ dB}) = 10$ dB is given as $P_r = 10^1 = 10$. Also, observe that given a power gain g, the received power is simply $P_r = gP_t$. Hence, for a received power $P_r > 10$, it naturally implies that

$$\begin{aligned} gP_t &> 10 \\ \Rightarrow g &> \frac{10}{P_t} = \frac{10}{20} \\ &= \frac{1}{2} \end{aligned}$$

Thus, the probability that the received power is greater than 10 essentially corresponds to the probability that the random power gain g of the Rayleigh fading wireless channel is greater than $\frac{1}{2}$. This probability can be readily computed as

$$\begin{aligned} \Pr\left(g > \frac{1}{2}\right) &= \int_{\frac{1}{2}}^{\infty} f_G(g)\, dg \\ &= \int_{\frac{1}{2}}^{\infty} e^{-g}\, dg \\ &= -e^{-g}\Big|_{\frac{1}{2}}^{\infty} \\ &= e^{-\frac{1}{2}} \\ &= 0.61 \end{aligned}$$

Qn 2 a

To gain a better understanding of the nature of the wireless environment and quantitatively analyze the performance of wireless communication systems, one needs to develop accurate analytical models to characterize them. In this section, we introduce the basic theory that deals with the analytical tools and techniques used extensively to model and assess wireless systems. In subsequent parts of the book, we build extensively on this theoretical framework to quantify the performance of various wireless communication schemes and systems. Let us start by considering the transmitted passband wireless signal $s(t)$, which is transmitted across

a wireless channel. Such a passband signal can be described analytically as,

$$s(t) = \mathrm{Re}\left\{ s_b\left(t\right) e^{j2\pi f_c t} \right\} \tag{3.1}$$

The quantity $s_b(t)$ is the complex baseband representation of the transmitted signal and f_c is simply the carrier frequency employed for transmission. Next, we need an analytical model for the wireless communication channel. To make things simple, we will assume initially that the wireless channel is time invariant. Let us consider a channel with L multipath components. Observe that each path of the wireless channel basically has two characteristic properties. Firstly, it delays the signal because of the propogation distance. Secondly, there is an attenuation of the signal arising because of the scattering effect. Let the signal attenuation and delay of the i^{th} channel be denoted by the quantities a_i, τ_i respectively. Recall from your knowledge of Linear Time Invariant (LTI) systems that the impulse response of an LTI system which attenuates a signal by a_i and delays it by τ_i is given as

$$h_i\left(\tau\right) = a_i \delta\left(\tau - \tau_i\right)$$

Hence, the above equation gives the impulse response of a single path of a wireless communication system. Further, observe that the wireless channel represents a linear input–output system, since the signal observed at the receiver is the sum of the different multipath signal copies impinging on the receive antenna. Therefore, a typical Channel Impulse Response (CIR) of a multipath-scattering based wireless channel is given by the sum of the above impulse responses corresponding to the individual model,

$$h\left(\tau\right) = \sum_{i=0}^{L-1} a_i \delta\left(\tau - \tau_i\right) \tag{3.2}$$

The above impulse response is also termed the *tapped delay-line* model because of the nature of the arrival of several progressively delayed components of the signal. It can be observed that the above wireless channel model consists of L propagation paths arising from the several reflection and scattering multipath *Non-Line-Of-Sight (NLOS)* components. One of the multipath components can also be a direct *Line-Of-Sight (LOS)* component. Each such i^{th} path is characterized by two parameters, which are,

1. The attenuation factor a_i
2. The path delay τ_i

Since the above wireless is a linear time-invariant (LTI) system, the received signal $y(t)$ can be expressed as the convolution of the transmitted signal $s\left(t\right)$ with the CIR $h\left(t\right)$. Therefore, the received wireless signal $y\left(t\right)$ is given as

$$y\left(t\right) = s\left(t\right) * h\left(t\right) = \int_{-\infty}^{\infty} h\left(\tau\right) s\left(t-\tau\right)\, d\tau$$

By inserting the expression for the tapped delay-line channel in Eq. (3.2) in the above convolution, the expression for the received wireless signal $y\left(t\right)$ across this tapped delay-line channel can be derived as

$$y\left(t\right) = \sum_{i=0}^{L-1} a_i \int_{-\infty}^{\infty} \delta\left(\tau-\tau_i\right) s\left(t-\tau\right)\, d\tau = \sum_{i=0}^{L-1} a_i s\left(t-\tau_i\right)\, d\tau$$

Further, this expression for the received signal can be written in terms of the transmitted baseband signal $s_b(t)$ by substituting the relation between $s(t)$ and $s_b(t)$ in Eq. (3.1) in the above expression and simplifying it as

$$y\left(t\right) = \mathrm{Re}\left\{\sum_{i=0}^{L-1} a_i s_b\left(t-\tau_i\right) e^{j2\pi f_c\left(t-\tau_i\right)}\right\}$$

$$= \mathrm{Re}\left\{\underbrace{\left(\sum_{i=0}^{L-1} a_i e^{-j2\pi f_c \tau_i} s_b\left(t-\tau_i\right)\right)}_{y_b(t)} e^{j2\pi f_c t}\right\}$$

From the above expression, it can readily be seen that $y_b\left(t\right)$, the complex baseband signal equivalent of the received signal $y\left(t\right)$, is simply given as

$$y_b\left(t\right) = \sum_{i=0}^{L-1} a_i e^{-j2\pi f_c \tau_i} s_b\left(t-\tau_i\right) \tag{3.3}$$

The different signal copies for a typical baseband BPSK information signal $s_b\left(t\right)$ is shown in Figure 3.2. The quantity T denotes the symbol time, while T_m, which is the *delay* between the first and last arriving copies of the signal, is termed the *delay spread*. This is an important parameter of the wireless channel and will be explored in detail in the next chapter. For the purpose of the discussion below and in the rest of the chapter we will assume a narrowband channel, i.e., one in which $T_m << T$. The above signal model will be further simplified in the following sections to yield meaningful insights into the performance of wireless communication systems.

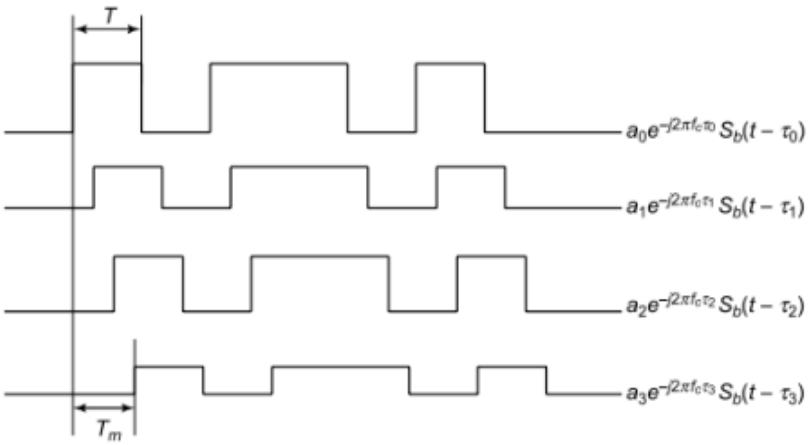

Figure 3.2 *Multipath signal components at the receiver*

Qn 2 b

Consider the instantaneous power $|h(\tau)|^2$ corresponding to the delay τ. The average power associated with this delay can be defined as

$$\phi(\tau) = \mathrm{E}\left\{|h(\tau)|^2\right\}$$

The above quantity $\phi(\tau)$ can be thought of as the average power associated with the delay τ at various instants of time. It can also be thought of as the power at delay τ for the wireless channels of different users in an area. The former is averaging over time, while the latter represents an averaging over the *ensemble* of channels. Similar to the framework in the previous section, one can define the fractional power associated with the delay τ as

$$f(\tau) = \frac{\phi(\tau)}{\int_0^\infty \phi(\tau)\, d\tau}$$

where $f(\tau)$ denotes the *power distribution density* corresponding to the delay τ, i.e., $f(\tau)\,\Delta\tau$ is the fraction of power in a delay interval of $\Delta\tau$ around τ. The average $\overline{\tau}$ can, therefore, be defined as

$$\overline{\tau} = \int_0^\infty \tau f(\tau)\, d\tau = \frac{\int_0^\infty \tau\phi(\tau)\, d\tau}{\int_0^\infty \phi(\tau)\, d\tau}$$

Finally, the RMS delay spread for the above power profile $\phi(\tau)$ is defined as

$$\sigma_\tau^{\mathrm{RMS}} = \sqrt{\int_0^\infty (\tau - \overline{\tau})^2 f(\tau)\, d\tau}$$

$$= \sqrt{\frac{\int_0^\infty (\tau - \overline{\tau})^2 \phi(\tau)\, d\tau}{\int_0^\infty \phi(\tau)\, d\tau}}$$

Qn 3 a

Property 1-Balance Property: Consider the BPSK-modulated PN sequence shown in Eq. (5.6). As already described, the PN sequence is of maximal length $2^D - 1 = 15$ corresponding to $D = 4$. Counting the number of -1 and $+1$ chips in the sequence, it can be seen that the number of -1s is *one* more than the number of $+1$s. This is termed the *balance* property of the PN sequence. This fundamentally arisies from the noiselike properties of PN sequences. If we are generating random noise of $+1,\ -1$ chips, with $P\left(X_i = +1\right) = P\left(X_i = -1\right) = \frac{1}{2}$, we expect to find on an average that *half* the chips are $+1$ and the rest are -1. In the above case, however, as the total number of chips is an odd number, i.e., 15, it is not possible to have an exactly even number of $+1,\ -1$s. Hence, we observe that the number of $+1,\ -1$s is close to half the total number, i.e., eight -1s and seven $+1$s. Thus, the balance property basically supports the notion of a noiselike PN chip sequence.

Property 2-Run-Length Property: A *run* is defined as a string of continuous values. There are a total of 8 runs in this PN sequences. For instance, the first run $-1,\ -1,\ -1,\ -1$ is a run of length 4. Thus, there is one run of length 4. Similarly, there is one run $+1,\ +1,\ +1$ of length 3, and two runs of length 2, viz., $-1,\ -1,\ +1,\ +1$. Finally, it can also be seen that there are 4 runs of length 1, viz., two runs of $+1$ and two runs of -1. Thus, there are a total of $2^{(D-1)} = 8$ runs. Out of the 8 runs, it can be seen that 1, i.e., $\frac{1}{8}$ of the runs are of length 3, $\frac{1}{4}$ of the runs are of length 2 and $\frac{1}{2}$ of the runs are of length 1. This is termed the *run-length* property of PN sequences and can be generalized as follows. Consider a maximal length PN sequence of length $2^D - 1$. Out of the total number of runs in the sequence, $\frac{1}{2}$ of the runs are of length 1, $\frac{1}{4}$ of the runs are of length 2, $\frac{1}{8}$ of the runs are of length 3, and so on. This is again in tune with the noiselike properties of PN sequences. For instance, consider a random IID sequence of $+1,\ -1$. In such a sequence, one would expect the average number of $+1$ or -1 to be half the total chips. Further, the number of strings $+1,\ +1$ or $-1,\ -1$, i.e., runs of length two would be expected to comprises $\frac{1}{4}$ of the total runs. This arises since the probability of seeing two

$$P\left(X_i = +1,\ X_{i+1} = +1\right) = \frac{1}{2} \times \frac{1}{2} = \frac{1}{4}$$

Similarly, one can explain the fraction $\frac{1}{8}$ corresponding to runs of length 3. Thus, this further supports the noiselike properties of PN sequences.

Property 3-Correlation Property: The *correlation* property is one of the most important properties of PN sequences. Consider again the BPSK chip sequence shown in Eq. (5.6) and denote it by $c_0\left(n\right)$. Let us now look at the correlation properties of this sequence. Consider the correlation $r_{00}\left(0\right)$, i.e., the correlation of the sequences c_0 with itself (the meaning of the (0) will become clear soon). This correlation is given as

$$\begin{aligned} r_{00}\left(0\right) &= \frac{1}{N}\sum_{i=0}^{N-1} c_0\left(n\right) c_0\left(n\right) \\ &= \frac{1}{N}\sum_{i=0}^{N-1} 1 \\ &= \frac{1}{N} \times N = 1 \end{aligned}$$

Now, consider a circularly shifted version of the PN sequence, shifted by $n_\circ = 2$. Let it be denoted by $c_0\left(n-2\right)$. This circularly shifted sequence by 2 chips can be readily seen to be given as

$$\begin{aligned} \text{PN Sequence} = &-1 + 1, -1 - 1 - 1 - 1 + 1 + 1 \\ &+1 - 1 + 1 + 1 - 1 - 1 + 1 \end{aligned} \tag{5.7}$$

Let us denote the correlation between $c_0\left(n\right)$ and $c_0\left(n-2\right)$ by $r_{00}\left(2\right)$, where the (2) can now be seen to represent a circular shift of 2. The correlation can be seen to be given as

$$r_{00}\left(2\right) = \frac{1}{N}\sum_{i=0}^{N-1} c_0\left(n\right) c_0\left(n-2\right)$$

Qn 3 b

Advantage 1: Jammer Margin

An important advantage of CDMA over conventional cellular systems is *jammer* suppression. A *jammer* is basically a malicious user in a communication network who transmits with a very high power to cause interference, thus leading to disruption of communication links. This is shown schematically in Figure 5.8. Jammers are of significant concern, especially in the context of highly secure communication systems such as those used for military and defense purposes. The effect of jammer suppression in a CDMA system can be understood as follows. Consider a communication system in which the signal $x\left(n\right)$ of the power P is received in the presence of additive white Gaussian noise $w\left(n\right)$ of power σ_w^2. The baseband system model for this communication system can be expressed as

$$y\left(n\right) = x\left(n\right) + w\left(n\right)$$

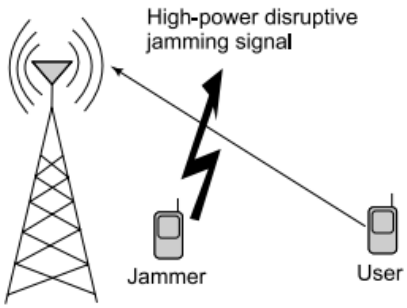

Figure 5.8 *Disruption by jammer in wireless communication*

Hence, the SNR at the receiver is $\text{SNR} = \frac{P}{\sigma_w^2}$. However, in the presence of a jamming signal $x_j(n)$ of power P_j, the received signal $y(n)$ is

$$y(n) = x(n) + x_j(n) + w(n)$$

Thus, the jammer interferes with the signal reception and the signal-to-interference-noise power ratio (SINR) can be calculated as $\text{SINR} = \frac{P}{P_j + \sigma_w^2}$. Thus, the jammer has a significant disruptive impact on the communication signal. Consider now a CDMA system in which the transmitted signal $x(n)$ is a spread-spectrum signal. As shown in the section above, the SINR for a CDMA scenario is given as

$$\text{SINR} = \frac{P}{\frac{P_j}{N} + \frac{\sigma_w^2}{N}} \tag{5.11}$$

Thus, it can be seen that the jamming power P_j is suppressed by a factor of N. Moreover, as the spreading factor N increases, the jammer suppression increases, minimizing the impact of the jammer on the communication system. This is termed *jammer suppression* in CDMA systems. Hence, CDMA which is inherently tolerant to jamming attacks is highly attractive for defense applications. In fact, the earliest applications of CDMA were in the context of tactical military secure communications, which were resistant to attacks by jammers. Only later were the benefits of CDMA realized and applied in the context of civilian cellular networks. Also, it is worthwhile noting that the gain of N in this context of jammer suppression is also termed the *jammer margin*. Thus, the jammer margin is equal to N, i.e., the spreading length of the CDMA codes.

Advantage 2: Graceful Degradation

Graceful degradation is another key property of CDMA-based wireless networks and as we shall see soon, allows for much more efficient interference management, which ultimately leads to universal frequency reuse and higher spectral efficiency. Consider the expression for the SINR at the user 0 derived in Eq. (5.10). At this point, assume that another user, i.e., a user with index $K+1$ joins the network. Let P_{K+1} denote the corresponding transmission power of this $(K+1)^{\text{th}}$ user and a_{K+1}, $c_{K+1}(n)$ denote his transmitted symbol and spreading code respectively. The SINR of the user 0 now changes to

$$\text{SINR} = \frac{P_0}{\frac{P_1}{N} + \frac{P_2}{N} + \ldots + \frac{P_K}{N} + \frac{P_{K+1}}{N} + \frac{\sigma_n^2}{N}}$$

$$= N \times \frac{P_0}{\sum_{k=0}^{K+1} P_k + \sigma_n^2}$$

Thus, the addition of a new user $K+1$ with power P_{K+1} only causes an incremental interference of $\frac{P_{K+1}}{N}$ at the user 0. Further, in general, at any user $i \neq (K+1)$, the additional interference due to the introduction of this new user is $\frac{P_{K+1}}{N}$. Therefore, the addition of the new user $K+1$ does not adversely affect any single user. Rather, the additional interference caused by this new user is *shared* amongst all the existing users in the system leading to *interference distribution*. This sharing of the interference by all the existing users leads to a *graceful degradation* of the SINR at each user. This is termed the *graceful degradation property of CDMA systems*. This idea of graceful degradation is key to understanding the big advantage of CDMA networks, i.e., *universal frequency reuse*, which is described next.

Qn 4 a

we consider a practical WiMAX example to illustrate the impact of the various parameters in the design of a complete OFDM system. As already stated in the beginning, WiMAX, which stands for Worldwide Interoperability for Microwave Access, is a prominent 4G wireless standard. The total number of subcarriers $N = 256$, with a bandwidth of 15.625 kHz per subcarrier. Therefore,

$$\frac{B}{N} = 15.625\,\text{kHz}$$

$$\Rightarrow B = N \times 15.625 = 256 \times 15.625$$

$$= 4\,\text{MHz}$$

Also, observe that the subcarrier bandwidth is less than the coherence bandwidth, i.e., $B_s = 15.625\,\text{kHz} << B_c = 250\,\text{kHz}$. Therefore, each subcarrier experiences frequency flat fading. The OFDM symbol time without CP is

$$\frac{N}{B} = \frac{256}{4 \times 10^6} = 64\,\mu s.$$

The raw OFDM symbol time, corresponding to the $N = 256$ IFFT samples, is $64\,\mu s$. WiMAX employs a cyclic prefix which is 12.5% of the symbol time. Therefore, the duration of the cylic prefix is

$$\text{Duration of cyclic prefix} = 12.5\% \text{ of symbol time}$$

$$= \frac{12.5}{100} \times 64\mu s,$$

$$= 8\ \mu s$$

Thus, the total transmitted OFDM symbol duration with cyclic prefix is $64\ \mu s + 8\ \mu s = 72\ \mu s$. Also, the number of samples in the CP is

$$\begin{aligned}\text{\# Samples in CP} &= \frac{\text{CP duration}}{\text{Sample time}} \\ &= \frac{8\ \mu s}{1/B} \\ &= 8\ \mu s \times 4 \times 10^6 \\ &= 32\end{aligned}$$

Thus, the length of the cyclic prefix $L_c = 32$ samples and the total number of samples is $256 + 32 = 288$. This break-up of the OFDM symbol in terms of the regular samples and the cyclic prefix is shown in Figure 7.11. Finally, the loss in spectral efficiency is

$$\begin{aligned}\text{Loss in spectral efficiency} &= \frac{32}{288} \\ &= \frac{8\ \mu s}{72\ \mu s} \\ &= 11.1\%\end{aligned}$$

This is the loss in spectral efficiency arising because of the addition of the cyclic prefix.

Qn 4 b

MIMO-OFDM is a combination of the Multiple-Input Multiple-Output (MIMO) wireless technology with that of OFDM, to further increase the rate in broadband multi-antenna wireless systems. Similar to OFDM, MIMO-OFDM converts a frequency-selective MIMO channel into multiple parallel flat fading MIMO channels. Hence, MIMO-OFDM significantly simplifies baseband receive processing by eliminating the need for a complex MIMO equalizer. We have already seen that the frequency-selective SISO channel is modelled as an FIR channel filter, with the output $y(n)$ at time instant n given as

$$\begin{aligned}y(n) &= \sum_{l=0}^{L-1} h(l)\, x(n-l) + w(n), \\ &= h(0)\, x(n) + \underbrace{h(1)\, x(n-1) + \ldots + h(L-1)\, x(n-L+1)}_{\text{ISI from previous symbols}} + w(n)\end{aligned}$$

where $w(n)$ denotes the noise. Hence, a MIMO frequency-selective channel can be modelled as a MIMO FIR filter, which can be described as

$$\begin{aligned}\mathbf{y}(n) &= \sum_{l=0}^{L-1} \mathbf{H}(l)\, x(n-l) + \mathbf{w}(n) \\ &= \mathbf{H}(0)\, x(n) + \underbrace{\mathbf{H}(1)\, x(n-1) + \ldots + \mathbf{H}(L-1)\, x(n-L+1)}_{\text{ISI from previous symbol vectors}} + \mathbf{w}(n)\end{aligned}$$

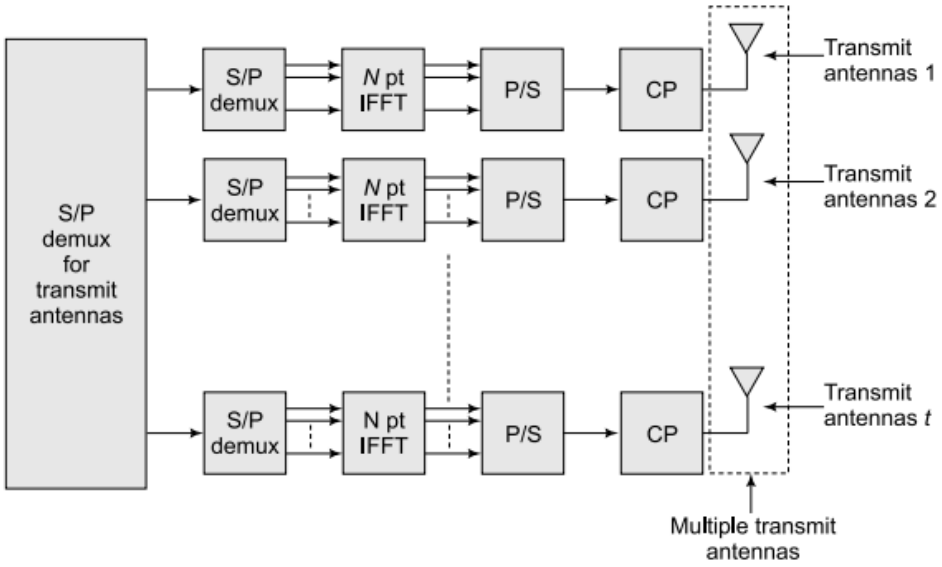

Figure 7.12 *MIMO OFDM transmitter schematic*

Therefore, the symbol vector $y(n)$ at the time instant n is affected by inter-symbol vector interference from $\mathbf{x}(n-1), \mathbf{x}(n-2), \ldots, \mathbf{x}(n-L+1)$. This is an L-tap frequency-selective MIMO channel. As can be seen, in a MIMO frequency-selective channel, the interference occurs between current and previous transmit symbol vectors. In a MIMO-OFDM system, one needs to perform the IFFT operation at each transmit antenna. The schematic figures showing clearly the processing at the transmitter and receiver of the MIMO-OFDM system are shown in figures 7.12 and 7.13 respectively. Hence, employing MIMO-OFDM, the MIMO frequency-selective channel can be converted into a set of parallel flat-fading MIMO channels.

These can be described as,

$$\tilde{\mathbf{y}}(0) = \tilde{\mathbf{H}}(0)\,\tilde{\mathbf{x}}(0)$$

$$\tilde{\mathbf{y}}(1) = \tilde{\mathbf{H}}(1)\,\tilde{\mathbf{x}}(1)$$

$$\vdots$$

$$\tilde{\mathbf{y}}(N-1) = \tilde{\mathbf{H}}(N-1)\,\tilde{\mathbf{x}}(N-1)$$

The model across the k^{th} subcarrier is $\tilde{\mathbf{y}}(k) = \tilde{\mathbf{H}}(k)\,\tilde{\mathbf{x}}(k)$, where $\tilde{\mathbf{y}}(k)$ and $\tilde{\mathbf{x}}(k)$ are the received and transmitted symbol vectors corresponding to the k^{th} subcarrier, and $\tilde{\mathbf{H}}(k)$ is the flat-fading channel matrix corresponding to the subcarrier k. Each of the received vectors $\tilde{\mathbf{y}}(0), \tilde{\mathbf{y}}(1), \ldots, \tilde{\mathbf{y}}(N-1)$ can be processed by a simple MIMO zero-forcing receiver or a MIMO-MMSE receiver for detection of the vectors $\tilde{\mathbf{x}}(0), \tilde{\mathbf{x}}(1), \ldots, \tilde{\mathbf{x}}(N-1)$. The zero-forcing MIMO receiver is given as

$$\hat{\tilde{\mathbf{x}}}_{\text{ZF}}(k) = \left(\tilde{\mathbf{H}}(k)\right)^{\dagger} \tilde{\mathbf{y}}(k)$$

$$= \left(\tilde{\mathbf{H}}^{H}(k)\,\tilde{\mathbf{H}}(k)\right)^{-1} \tilde{\mathbf{H}}^{H}(k)\,\tilde{\mathbf{y}}(k)$$

Qn 5 a

In 1982, many European countries came together under the auspices of the Conference of European Posts and Telegraphs (CEPT) to develop and standardize a pan-European system for mobile services. The group was called the Groupe Spécial Mobile (GSM) and their main charter was to develop a system that could deliver inexpensive wireless voice services, and work seamlessly across all of Europe. Prior to GSM, the European cellular market was fragmented with a variety of mutually incompatible systems deployed in different countries: Scandinavian countries had NMT-400 and NMT-900, Germany had C-450, the United Kingdom had TACS, and France had Radiocom.

By 1989, the European Telecommunications Standards Institute (ETSI) took over the development of the GSM standard and the first version, called GSM Phase I, was released in 1990. Shortly thereafter, several operators in Europe deployed GSM. GSM quickly gained acceptance beyond Europe and the standard was appropriately renamed as the Global System for Mobile Communications. According to the Informa Telecoms and Media, an industry analyst, GSM and its successor technologies today boast over 4.2 billion subscribers spread across 220 countries, a 90% global market share. The broad worldwide adoption of GSM has made international roaming a seamless reality.

The GSM air-interface is based on a TDMA scheme where eight users are multiplexed on a single 200kHz wide frequency channel by assigning different time slots to each user. GSM employed a variant of FSK called Gaussian Minimum Shift Keying (GMSK) as its modulation technique. GMSK was chosen due to its constant envelope property providing good power and spectral efficiency characteristics.

Besides voice and SMS, the original GSM standard also supported circuit-switched data at 9.6kbps. By the mid-1990s, ETSI introduced the GSM Packet Radio Systems (GPRS) as an evolutionary step for GSM systems toward higher data rates. GPRS and GSM systems share the same frequency bands, time slots, and signaling links. GPRS defined four different channel coding schemes supporting 8kbps to 20kbps per slot. Under favorable channel conditions, the higher 20kbps rate can be used, and if all eight slots in the GSM TDM frame were used for data transmission, in theory, GPRS could provide a maximum data rate of 160kbps. Typical implementations of GPRS provided a user data rate of 20–40kbps.

Figure 1.2 provides a high-level architecture of a GSM/GPRS network. It is instructive to review this architecture as it formed the basis from which later 3G systems and LTE evolved. The original GSM architecture had two sub-components:

- **Base Station Subsystem**: This is comprised of the base-station transceiver (BTS) units that the mobile stations (MS) connect with over the air-interface and the base station controller (BSC), which manages and aggregates traffic from several BTSs for transport to the switching core, and manages mobility across BTSs connected directly to them. BSCs evolved to become Radio Network Controllers (RNC) in the 3G evolution of GSM.
- **Network Switching Sub-system**: This is comprised of the Mobile Switching Center (MSC) and subscriber data bases. The MSC provides the required switching to connect the calling party with the called party and is interconnected with the Public Switched Telephone Network (PSTN). The MSC uses the Home Location Register (HLR) and Visitor Location Register (VLR) to determine the location of mobile subscribers for call control purposes.

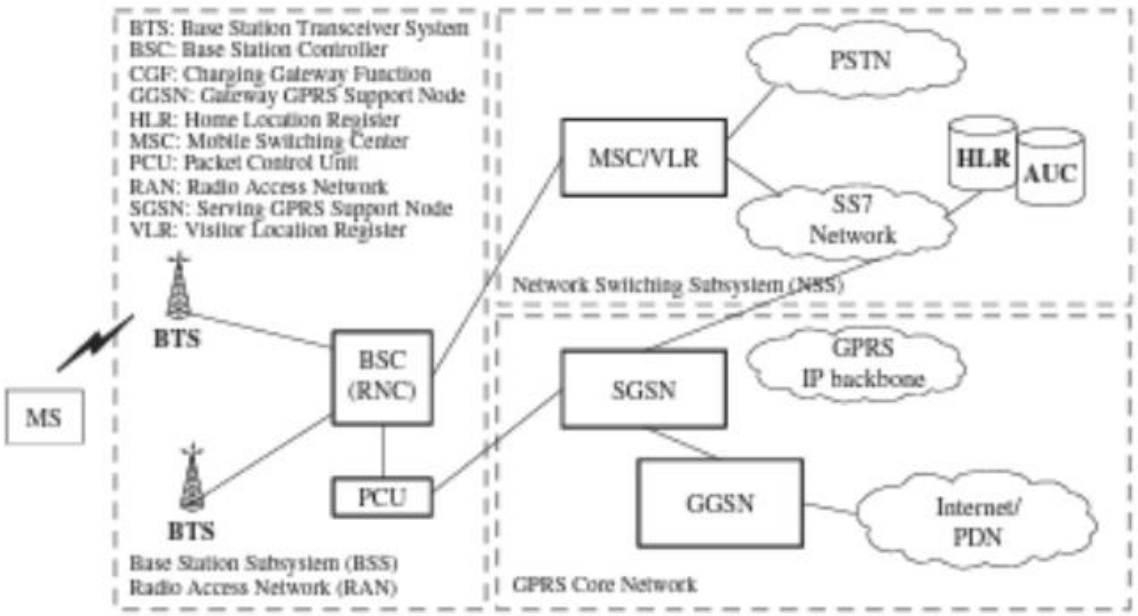

Figure 1.2 GSM network architecture.

Qn 5 b

Figure 1.3 shows how the 3GPP network architecture evolved over a few releases. 3GPP Release 6 architecture, which is conceptually very similar to its predecessors, has four network elements in the data path: the base station or Node-B, radio network controller (RNC), serving GPRS service node (SGSN), and gateway GRPS service node (GGSN). Release 7 introduced a direct tunnel option from the RNC to GGSN, which eliminated SGSN from the data path. LTE on the other hand, will have only two network elements in the data path: the enhanced Node-B or eNode-B, and a System Architecture Evolution Gateway (SAE-GW). Unlike all previous cellular systems, LTE merges the base station and radio network controller functionality into a single unit. The control path includes a functional entity called the Mobility Management Entity (MME), which provides control plane functions related to subscriber, mobility, and session management. The MME and SAE-GW could be collocated in a single entity called the access gateway (a-GW). More details about the network architecture are provided in the next section.

A key aspect of the LTE flat architecture is that all services, including voice, are supported on the IP packet network using IP protocols. Unlike previous systems, which had a separate circuit-switched subnetwork for supporting voice with their own Mobile Switching Centers (MSC) and transport networks, LTE envisions only a single evolved packet-switched core, the EPC, over which all services are supported, which could provide huge operational and infrastructure cost savings. It should be noted, however, that although LTE has been designed for IP services with a flat architecture, due to backwards compatibility reasons certain legacy, non-IP aspects of the 3GPP architecture such as

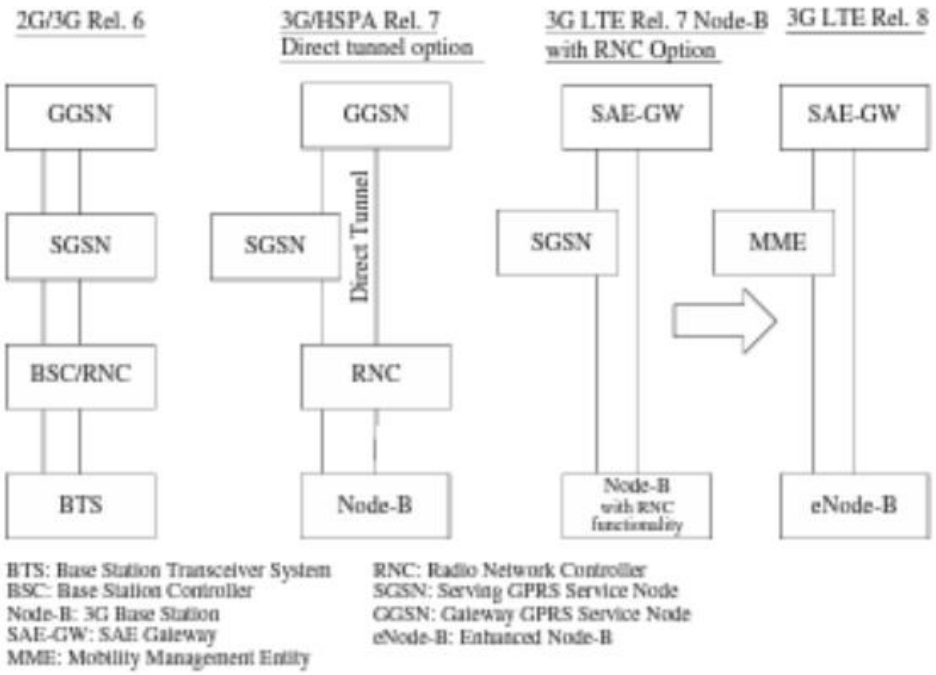

Figure 1.3 3GPP evolution toward a flat LTE SAE architecture.

the GPRS tunneling protocol and PDCP (packet data convergence protocol) still exists within the LTE network architecture.

Qn 6 a

The LTE standard provides extensive support for implementing advanced multiantenna solutions to improve link robustness, system capacity, and spectral efficiency. Depending on the deployment scenario, one or more of the techniques can be used. Multiantenna techniques supported in LTE include:

- **Transmit diversity**: This is a technique to combat multipath fading in the wireless channel. The idea here is to send copies of the same signal, coded differently, over multiple transmit antennas. LTE transmit diversity is based on space-frequency block coding (SFBC) techniques complemented with frequency shift time diversity (FSTD) when four transmit antenna are used. Transmit diversity is primarily intended for common downlink channels that cannot make use of channel-dependent scheduling. It can also be applied to user transmissions such as low data rate VoIP, where the additional overhead of channel-dependent scheduling may not be justified. Transmit diversity increases system capacity and cell range.
- **Beamforming**: Multiple antennas in LTE may also be used to transmit the same signal appropriately weighted for each antenna element such that the effect is to focus the transmitted beam in the direction of the receiver and away from interference, thereby improving the received signal-to-interference ratio. Beamforming can provide significant improvements in coverage range, capacity, reliability, and battery life. It can also be useful in providing angular information for user tracking. LTE supports beamforming in the downlink.

- **Multi-user MIMO**: Since spatial multiplexing requires multiple transmit chains, it is currently not supported in the uplink due to complexity and cost considerations. However, multi-user MIMO (MU-MIMO), which allows multiple users in the uplink, each with a single antenna, to transmit using the same frequency and time resource, is supported. The signals from the different MU-MIMO users are separated at the base station receiver using accurate channel state information of each user obtained through uplink reference signals that are orthogonal between users.

Qn 6 b

The EPC includes four new elements: (1) Serving Gateway (SGW), which terminates the interface toward the 3GPP radio access networks; (2) Packet Data Network Gateway (PGW), which controls IP data services, does routing, allocates IP addresses, enforces policy, and provides access for non-3GPP access networks; (3) Mobility Management Entity (MME), which supports user equipment context and identity as well as authenticates and authorizes users; and (4) Policy and Charging Rules Function (PCRF), which manages QoS aspects. Figure 1.4 shows the end-to-end architecture including how the EPC supports LTE as well as current and legacy radio access networks.

A brief description of each of the four new elements is provided here:

- **Serving Gateway (SGW)**: The SGW acts as a demarcation point between the RAN and core network, and manages user plane mobility. It serves as the mobility anchor when terminals move across areas served by different eNode-B elements in E-UTRAN, as well as across other 3GPP radio networks such as GERAN and UTRAN. SGW does downlink packet buffering and initiation of network-triggered service request procedures. Other functions include lawful interception, packet routing and forwarding, transport level packet marking in the uplink and the downlink, accounting support for per user, and inter-operator charging.

- **Packet Data Network Gateway (PGW)**: The PGW acts as the termination point of the EPC toward other Packet Data Networks (PDN) such as the Internet, private IP network, or the IMS network providing end-user services. It serves as an anchor point for sessions toward external PDN and provides functions such as user IP address allocation, policy enforcement, packet filtering, and charging support. Policy enforcement includes operator-defined rules for resource allocation to control data rate, QoS, and usage. Packet filtering functions include deep packet inspection for application detection.

- **Policy and Charging Rules Function (PCRF)**: The Policy and Charging Rules Function (PCRF) is a concatenation of Policy Decision Function (PDF) and Charging Rules Function (CRF). The PCRF interfaces with the PDN gateway and supports service data flow detection, policy enforcement, and flow-based charging. The PCRF was actually defined in Release 7 of 3GPP ahead of LTE. Although not much deployed with pre-LTE systems, it is mandatory for LTE. Release 8 further enhanced PCRF functionality to include support for non-3GPP access (e.g., Wi-Fi or fixed line access) to the network.

Qn 7a

Consider a MIMO wireless system with t transmit antennas and r receive antennas. Such a MIMO system is also termed an $r \times t$ system. Let $x_1, x_2, \ldots, x_t$ denote the t symbols transmitted from the t transmit antennas in the MIMO system, i.e., x_i denotes the symbol transmitted from the i^{th} transmit antenna $1 \leq i \leq t$. These transmit symbols can be stacked to form the t-dimensional vector, also termed the *transmit vector*,

$$\mathbf{x} = \begin{bmatrix} x_1 \\ x_2 \\ \vdots \\ x_t \end{bmatrix}$$

Corresponding to this transmission, let $y_1, y_2, \ldots, y_t$ denote the r received symbols across the r receive antennas in the MIMO systems, which can be stacked as the r-dimensional receive symbol vector,

$$\mathbf{y} = \begin{bmatrix} y_1 \\ y_2 \\ \vdots \\ y_r \end{bmatrix}$$

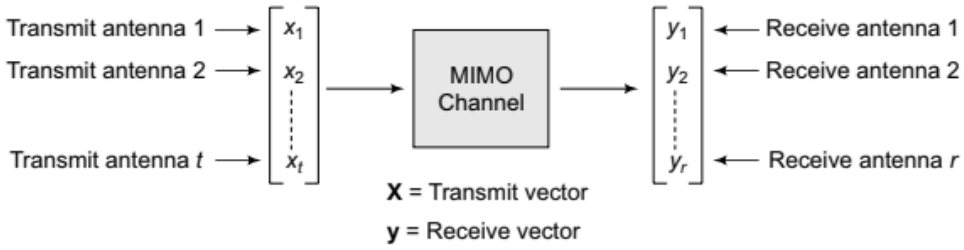

Figure 6.2 *MIMO system input-output schematic*

This is shown schematically in Figure 6.2. Let the complex coefficient h_{ij} represent the fading channel coefficient between the i^{th} receive antenna and the j^{th} transmit antenna. Thus, there are a net of rt channel coefficients in this wireless scenario corresponding to all possible combinations of the r receive antennas and t transmit antennas. These can be arranged in a matrix form as

$$\mathbf{H} = \begin{bmatrix} h_{11} & h_{12} & \ldots & h_{1t} \\ h_{21} & h_{22} & \ldots & h_{2t} \\ \vdots & \vdots & \ddots & \vdots \\ h_{r1} & h_{r2} & \ldots & h_{rt} \end{bmatrix}$$

where the $r \times t$ dimensional matrix $\mathbf{H}$ is termed the MIMO channel matrix. Let the additive noise at the receive antenna i be denoted by n_i, i.e., $n_1, n_2, \ldots, n_r$ denote the additive noise at the r receive antennas. Thus, the net MIMO input output system model can be represented in vector form as

$$\underbrace{\begin{bmatrix} y_1 \\ y_2 \\ \vdots \\ y_r \end{bmatrix}}_{\mathbf{y}} = \underbrace{\begin{bmatrix} h_{11} & h_{12} & \ldots & h_{1t} \\ h_{21} & h_{22} & \ldots & h_{2t} \\ \vdots & \vdots & \ddots & \vdots \\ h_{r1} & h_{r2} & \ldots & h_{rt} \end{bmatrix}}_{\mathbf{H}} \underbrace{\begin{bmatrix} x_1 \\ x_2 \\ \vdots \\ x_t \end{bmatrix}}_{\mathbf{x}} + \underbrace{\begin{bmatrix} n_1 \\ n_2 \\ \vdots \\ n_r \end{bmatrix}}_{\mathbf{n}}$$

This is succinctly represented using matrix notation as

$$\mathbf{y} = \mathbf{H}\mathbf{x} + \mathbf{n}$$

Observe that the receive symbol y_1 is given as

$$y_1 = h_{11}x_1 + h_{12}x_2 + \ldots + h_{1t}x_t + n_1$$

from which it can be seen that all the symbols $x_1, x_2, \ldots, x_t$ interfere at y_1 received at the receive antenna 1. Similarly, the receive symbol y_2 is given as

$$y_2 = h_{21}x_2 + h_{22}x_2 + \ldots + h_{2t}x_t + n_2$$

from which it can be once again seen that $x_1, x_2, \ldots, x_t$ interfere at y_2 received at the receive antenna 2. This is, in general, true for all the receive antennas, i.e., at each receive antenna i, the receive symbol y_i is a linear of all the transmit symbols $x_1, x_2, \ldots, x_t$ from the t transmit antennas, observed in additive noise n_i. For the special case of $t = 1$, i.e., single transmit antenna and multiple receive antennas, this is termed as *Single-Input Multiple-Output (SIMO)* system or the receive diversity system as seen earlier. This can be modelled as

$$\underbrace{\begin{bmatrix} y_1 \\ y_2 \\ \vdots \\ y_r \end{bmatrix}}_{\mathbf{y}} = \underbrace{\begin{bmatrix} h_1 \\ h_2 \\ \vdots \\ h_r \end{bmatrix}}_{\mathbf{h}} x + \underbrace{\begin{bmatrix} n_1 \\ n_2 \\ \vdots \\ n_r \end{bmatrix}}_{\mathbf{n}}$$

Similarly, for the case of one receive antenna, i.e., $r = 1$ and multiple transmit antennas, it is termed a *Multiple-Input Single-Output (MISO) system* model or a transmit diversity system. Its system model is given as

$$y = \underbrace{\begin{bmatrix} h_1 & h_1 & \dots & h_t \end{bmatrix}}_{\mathbf{h}^T} \underbrace{\begin{bmatrix} x_1 \\ x_2 \\ \vdots \\ x_t \end{bmatrix}}_{\mathbf{x}} + n$$

Finally, for $r = t = 1$, i.e., a single receive and transmit antenna, it reduces to the single-input single-output (SISO) system, modelled as

$$y = hx + n$$

As the reader might recall, this was the first system model that was introduced to model the Rayleigh fading wireless -channel-based wireless communication. The *covariance* matrix of the noise $\mathbf{R_n}$ of the noise vector $\mathbf{n}$ defined as

$$\begin{aligned}
\mathbf{R_n} &= \mathrm{E}\left\{\mathbf{n}\mathbf{n}^H\right\} \\
&= \mathrm{E}\left\{\begin{bmatrix} n_1 \\ n_2 \\ \vdots \\ n_L \end{bmatrix} \begin{bmatrix} n_1^* & n_2^* & \dots & n_L^* \end{bmatrix}\right\} \\
&= \begin{bmatrix} \mathrm{E}\left\{|n_1|^2\right\} & \mathrm{E}\{n_1 n_2^*\} & \dots & \mathrm{E}\{n_1 n_r^*\} \\ \mathrm{E}\{n_2 n_1^*\} & \mathrm{E}\left\{|n_2|^2\right\} & \dots & \mathrm{E}\{n_2 n_r^*\} \\ \vdots & \vdots & \ddots & \vdots \\ \mathrm{E}\{n_r n_1^*\} & \mathrm{E}\{n_r n_2^*\} & \dots & \mathrm{E}\left\{|n_r|^2\right\} \end{bmatrix} \\
&= \begin{bmatrix} \sigma_n^2 & 0 & 0 & \dots & 0 \\ 0 & \sigma_n^2 & 0 & \dots & 0 \\ \vdots & \vdots & \vdots & \ddots & \vdots \\ 0 & 0 & 0 & \dots & \sigma_n^2 \end{bmatrix} \\
&= \sigma_n^2 \mathbf{I}_r
\end{aligned}$$

The noise vector $\mathbf{n}$ with the covariance structure above is termed *spatially* uncorrelated additive noise, since the noise samples at the different antennas i, j are independent, i.e., $\mathrm{E}\left\{n_i n_j^*\right\} = 0$ if $i \neq j$. Finally, to denote the transmission and reception across different time instants, one can add the time index k to the MIMO system model to frame the net model as

$$\underbrace{\begin{bmatrix} y_1(k) \\ y_2(k) \\ \vdots \\ y_r(k) \end{bmatrix}}_{\mathbf{y}(k)} = \underbrace{\begin{bmatrix} h_{11} & h_{12} & \dots & h_{1t} \\ h_{21} & h_{22} & \dots & h_{2t} \\ \vdots & \vdots & \ddots & \vdots \\ h_{r1} & h_{r2} & \dots & h_{rt} \end{bmatrix}}_{\mathbf{H}} \underbrace{\begin{bmatrix} x_1(k) \\ x_2(k) \\ \vdots \\ x_t(k) \end{bmatrix}}_{\mathbf{x}(k)} + \underbrace{\begin{bmatrix} n_1(k) \\ n_2(k) \\ \vdots \\ n_r(k) \end{bmatrix}}_{\mathbf{n}(k)}$$

Thus, the vectors $\mathbf{y}(k)$, $\mathbf{x}(k)$, $\mathbf{n}(k)$ define the receive, transmit, and noise vectors of the MIMO wireless communication system at the time instant k. Notice that above we have assumed the channel matrix $\mathbf{H}$ to be constant or, in other words, not dependent on the time instant k. This is also termed a slow fading or *quasi-static* channel matrix, indicating that the channel coefficients are constant over the block of MIMO vectors that are transmitted. Lastly, we also assume that any two noise samples across two different time instants are uncorrelated, i.e., $\mathrm{E}\left\{n_i(k)\, n_j^*(l)\right\} = 0$ if $k \neq l$. Hence, the noise covariance matrix is given as

$$\mathrm{E}\left\{\mathbf{n}(k)\, \mathbf{n}(l)^H\right\} = \sigma^2 \delta(k-l)\, \mathbf{I}_r$$

where the delta function $\delta(k-l) = 1$ if $k = l$ and 0 otherwise.

Qn 7 b

This can be considered as solving the system of linear equations,

$$\mathbf{y} = \mathbf{H}\mathbf{x}$$

where $x_1, x_2, \dots, x_t$ are the t unknowns and there are r equations corresponding to the r observations $y_1, y_2, \dots, y_r$. Consider a simplistic scenario, where $r = t$, i.e., the number of receive antennas is equal to the number of transmit antennas. In this case, the matrix $\mathbf{H}$ is square. Further, if the matrix $\mathbf{H}$ is now invertible, the estimate $\hat{\mathbf{x}}$ of the transmit vector $\mathbf{x}$ is still given as

$$\hat{\mathbf{x}} = \mathbf{H}^{-1}\hat{\mathbf{y}}$$

However, frequently, one has more receive antennas than transmit antennas, i.e., $r > t$. In this scenario, the system $\mathbf{y} = \mathbf{H}\mathbf{x}$ is given as

$$\underbrace{\begin{bmatrix} y_1(k) \\ y_2(k) \\ \vdots \\ \vdots \\ \vdots \\ y_r(k) \end{bmatrix}}_{\mathbf{y}(k)} = \underbrace{\begin{bmatrix} h_{11} & h_{12} & \dots & h_{1t} \\ h_{21} & h_{22} & \dots & h_{2t} \\ \vdots & \vdots & \ddots & \vdots \\ \vdots & \vdots & \ddots & \vdots \\ \vdots & \vdots & \ddots & \vdots \\ h_{r1} & h_{r2} & \dots & h_{rt} \end{bmatrix}}_{\mathbf{H}} \underbrace{\begin{bmatrix} x_1(k) \\ x_2(k) \\ \vdots \\ x_t(k) \end{bmatrix}}_{\mathbf{x}(k)}$$

from which it can be seen that the matrix $\mathbf{H}$ has more rows than columns. Such a matrix is popularly known as a *tall* matrix due to its structure. In this situation, one cannot exactly solve for $\mathbf{x}$ since there are more equations r than unknowns t. Hence, one can resort to choosing the vector $\mathbf{x}$ which minimizes the estimation error error $f(\hat{\mathbf{x}})$,

$$f(\mathbf{x}) = \|\mathbf{y} - \mathbf{H}\mathbf{x}\|^2$$

The above error function is also termed the *least-squares* error function and the resulting estimator is termed the *least-squares estimator*. To simplify the analysis going forward, we consider real vectors/matrices $\mathbf{y}, \mathbf{x}, \mathbf{H}$. The case for complex quantities will be dealt later. The above error function can be expanded as

$$\begin{aligned} f(\mathbf{x}) &= \|\mathbf{y} - \mathbf{H}\mathbf{x}\|^2, \\ &= (\mathbf{y} - \mathbf{H}\mathbf{x})^T (\mathbf{y} - \mathbf{H}\mathbf{x}) \\ &= \left(\mathbf{y}^T - \mathbf{x}^T\mathbf{H}^T\right)(\mathbf{y} - \mathbf{H}\mathbf{x}) \\ &= \mathbf{y}^T\mathbf{y}^T - \mathbf{x}^T\mathbf{H}^T\mathbf{y} - \mathbf{y}^T\mathbf{H}\mathbf{x} + \mathbf{x}^T\mathbf{H}^T\mathbf{H}\mathbf{x} \\ &= \mathbf{y}^T\mathbf{y} - 2\mathbf{x}^T\mathbf{H}^T\mathbf{y} + \mathbf{x}^T\mathbf{H}^T\mathbf{H}\mathbf{x} \end{aligned} \tag{6.1}$$

where we have used the relation $\mathbf{y}^T\mathbf{H}\mathbf{x} = \left(\mathbf{y}^T\mathbf{H}\mathbf{x}\right)^T = \hat{\mathbf{x}}^T\mathbf{H}^T\mathbf{y}$ in the above simplification. This is due to the fact that $\mathbf{y}^T\mathbf{H}\mathbf{x}$ is a scalar and, hence, is equal to its transpose. To find the minimum of the error function $f(\mathbf{x})$ with respect to $\mathbf{x}$, we have to set the derivative with respect to $\mathbf{x}$ equal to 0. For this purpose, the concept of a vector derivative is briefly described below. Consider a multidimensional function $g(\mathbf{x})$. The vector derivative of $g(\mathbf{x})$ with respect to $\mathbf{x}$ is defined as

$$\frac{\partial g(\mathbf{x})}{\partial \mathbf{x}} = \begin{bmatrix} \frac{\partial g(\mathbf{x})}{\partial x_1} \\ \frac{\partial g(\mathbf{x})}{\partial x_2} \\ \vdots \\ \frac{\partial g(\mathbf{x})}{\partial x_t} \end{bmatrix}$$

which is basically a t-dimensional vector with the i^{th} component equal to the derivative of $f(\mathbf{x})$ with respect to x_i. This can be better understood with the aid of an example. Consider any vector $\mathbf{c} = [c_1, c_2, \ldots, c_t]^T$. Let the function $g(\mathbf{x})$ be defined as

$$g(\mathbf{x}) = \mathbf{c}^T\mathbf{x} = c_1x_1 + c_2x_2 + \ldots + c_tx_t$$

$$\frac{\partial g(\mathbf{x})}{\partial \mathbf{x}} = \begin{bmatrix} \frac{\partial g(\mathbf{x})}{\partial x_1} \\ \frac{\partial g(\mathbf{x})}{\partial x_2} \\ \vdots \\ \frac{\partial g(\mathbf{x})}{\partial x_t} \end{bmatrix} = \begin{bmatrix} c_1 \\ c_2 \\ \vdots \\ c_t \end{bmatrix} = \mathbf{c}$$

$$\frac{\partial f(\mathbf{x})}{\mathbf{x}}\bigg|_{\mathbf{x}=\hat{\mathbf{x}}} = 0$$

$$-2\mathbf{H}^T\mathbf{y} + 2\mathbf{H}^T\mathbf{H}\hat{\mathbf{x}} = 0$$

$$\mathbf{H}^T\mathbf{H}\hat{\mathbf{x}} = \mathbf{H}^T\mathbf{y}$$

$$\hat{\mathbf{x}} = \left(\mathbf{H}^T\mathbf{H}\right)^{-1}\mathbf{H}^T\mathbf{y}$$

The above decoder for the MIMO wireless system to decode the transmitted symbol vector $\mathbf{x}$ from the received symbol vector $\mathbf{y}$ is termed the *zero-forcing receiver* or simply the *ZF receiver*. Hence, the zero-forcing decoder can be expressed as

$$\hat{\mathbf{x}}_{\text{ZF}} = \underbrace{\left(\mathbf{H}^H\mathbf{H}\right)^{-1}\mathbf{H}^H}_{\mathbf{F}_{\text{ZF}}}\mathbf{y} \tag{6.2}$$

The matrix $\mathbf{F}_{\text{ZF}} = \left(\mathbf{H}^H\mathbf{H}\right)^{-1}\mathbf{H}^H$ is also termed the *zero-forcing receiver matrix* and the estimate $\hat{\mathbf{x}}_{\text{ZF}}$ is, therefore, given as

$$\hat{\mathbf{x}}_{\text{ZF}} = \mathbf{F}_{\text{ZF}}\mathbf{y}$$

Qn 8 a

$$\underbrace{\begin{bmatrix} y_1 \\ y_2 \\ y_3 \end{bmatrix}}_{\mathbf{y}} = \underbrace{\begin{bmatrix} 2 & 3 \\ 1 & 3 \\ 4 & 2 \end{bmatrix}}_{\mathbf{H}} \underbrace{\begin{bmatrix} x_1 \\ x_2 \end{bmatrix}}_{\mathbf{x}} + \underbrace{\begin{bmatrix} n_1 \\ n_2 \\ n_3 \end{bmatrix}}_{\mathbf{n}}$$

Thus, as can be seen from the model above, the transmit vector $\mathbf{x}$ is of dimension 2×1, while the receive and noise vectors $\mathbf{y}$, $\mathbf{n}$ respectively are of dimension 3×1. The above MIMO system model can also be explicitly written to describe the signal received at each receive antenna as

$$y_1 = 2x_1 + 3x_2 + n_1$$

$$y_2 = x_1 + 3x_2 + n_2$$

$$y_3 = 4x_1 + 2x_2 + n_3$$

$$\mathbf{H}^H\mathbf{H} = \begin{bmatrix} 2 & 1 & 4 \\ 3 & 3 & 2 \end{bmatrix} \begin{bmatrix} 2 & 3 \\ 1 & 3 \\ 4 & 2 \end{bmatrix}$$

$$= \begin{bmatrix} 21 & 17 \\ 17 & 22 \end{bmatrix}$$

Hence, the expression for $\left(\mathbf{H}^H\mathbf{H}\right)^{-1}$ can be simplified as

$$\left(\mathbf{H}^H\mathbf{H}\right)^{-1} = \frac{1}{21 \times 22 - 17 \times 17} \begin{bmatrix} 22 & -17 \\ -17 & 21 \end{bmatrix}$$

$$= \frac{1}{173} \begin{bmatrix} 22 & -17 \\ -17 & 21 \end{bmatrix}$$

Thus, the zero-forcing receiver matrix $\mathbf{F}_{ZF} = \left(\mathbf{H}^H\mathbf{H}\right)^{-1}\mathbf{H}^H$ can be expressed as

$$\begin{aligned} \mathbf{F}_{ZF} &= \left(\mathbf{H}^H\mathbf{H}\right)^{-1}\mathbf{H}^H \\ &= \frac{1}{173} \begin{bmatrix} 22 & -17 \\ -17 & 21 \end{bmatrix} \begin{bmatrix} 2 & 1 & 4 \\ 3 & 3 & 2 \end{bmatrix} \\ &= \frac{1}{173} \begin{bmatrix} -7 & -29 & 54 \\ 29 & 46 & -26 \end{bmatrix} \\ &= \begin{bmatrix} -0.04 & -0.17 & 0.31 \\ 0.17 & 0.27 & -0.15 \end{bmatrix} \end{aligned} \tag{6.5}$$

Thus, the zero-forcing estimate of the transmit vector is given as

$$\begin{aligned} \hat{\mathbf{x}}_{\text{ZF}} &= \mathbf{F}_{ZF}\mathbf{y} \\ &= \left(\mathbf{H}^H\mathbf{H}\right)^{-1}\mathbf{H}^H\mathbf{y} \end{aligned}$$

$$= \begin{bmatrix} -0.04 & -0.17 & 0.31 \\ 0.17 & 0.27 & -0.15 \end{bmatrix} \begin{bmatrix} y_1 \\ y_2 \\ y_3 \end{bmatrix}$$

These expressions can now be explicitly written for the estimate of each of the transmit symbols $\hat{x}_1$, $\hat{x}_2$ as

$$\hat{x}_1 = -0.04y_1 - 0.17y_2 + 0.31y_3$$

$$\hat{x}_2 = +0.17y_1 + 0.27y_2 - 0.15y_3$$

Qn 8 b

In this section, we develop the *Minimum Mean-Squared Error (MMSE)* receiver for the MIMO wireless communication system. The MMSE receiver is based on a *Bayesian* approach, meaning that the transmit vector $\mathbf{x}$ is assumed to be random in nature. Thus, if $\hat{\mathbf{x}}_{\text{MMSE}}$ denotes the estimated symbol vector, the MMSE receiver minimizes the average or mean of the squared error

$$\mathrm{E}\left\{\|\hat{\mathbf{x}}_{\text{MMSE}} - \mathbf{x}\|^2\right\}$$

Thus, it is aptly named minimum mean-squared error estimator. To illustrate the development of the MMSE receiver, we consider a single-input multiple-output (SIMO) wireless system, i.e., $t = 1$, and generalize the result to the case of a MIMO system. Hence, consider the SIMO system model given as

$$\mathbf{y} = \mathbf{h}x + \mathbf{n}$$

where x is now a scalar transmitted symbol. Thus, the basic problem can be interpreted as estimating the symbol x given the vector $\mathbf{y} = [y_1, y_2, \ldots, y_r]^T$. Let $\mathbf{c} = [c_1, c_2, \ldots, c_r]^T$. One can now define a linear estimator of x as

$$\hat{x} = \mathbf{c}^T\mathbf{y} \tag{6.7}$$

$$= \begin{bmatrix} c_1 & c_2 & \ldots & c_r \end{bmatrix} \begin{bmatrix} y_1 \\ y_2 \\ \vdots \\ y_r \end{bmatrix}$$

$$= c_1y_1 + c_2y_2 + \ldots + c_ry_r$$

Such an estimator as above is termed as a *linear* estimator, since the estimate is a linear function of $\mathbf{y}$. We now wish to find the best or optimal linear estimator $\hat{\mathbf{x}}_{\text{MMSE}}$, which minimizes the mean squared error and hence is also termed the *Linear Minimum Mean Squared Estimator (LMMSE)*. This is frequently also referred to simply as the MMSE, although strictly speaking belongs to the specific class of linear estimators. The average mean squared error is defined as

$$\mathrm{E}\left\{\|\hat{\mathbf{x}}-\mathbf{x}\|^2\right\}$$

Employing the form in Eq. (6.7), the resulting equation can be simplified as

$$\begin{aligned}
\mathrm{E}\left\{\|\hat{\mathbf{x}}-\mathbf{x}\|^2\right\} &= \mathrm{E}\left\{\left(\mathbf{c}^T\mathbf{y}-\mathbf{x}\right)\left(\mathbf{c}^T\mathbf{y}-\mathbf{x}\right)^T\right\} \\
&= \mathrm{E}\left\{\left(\mathbf{c}^T\mathbf{y}-\mathbf{x}\right)\left(\mathbf{y}^T\mathbf{c}-\mathbf{x}^T\right)\right\} \\
&= \mathrm{E}\left\{\mathbf{c}^T\mathbf{y}\mathbf{y}^T\mathbf{c}-x\mathbf{y}^T\mathbf{c}-\mathbf{c}^T\mathbf{y}x+xx^T\right\} \\
&= \mathbf{c}^T\underbrace{\mathrm{E}\left\{\mathbf{y}\mathbf{y}^T\right\}}_{\mathbf{R}_{yy}}\mathbf{c}-\underbrace{\mathrm{E}\left\{x\mathbf{y}^T\right\}}_{\mathbf{R}_{xy}}\mathbf{c}-\mathbf{c}^T\underbrace{\mathrm{E}\left\{\mathbf{y}x\right\}}_{\mathbf{R}_{yx}}+\mathrm{E}\left\{x^2\right\}_{\mathbf{R}_{xx}} \\
&= \mathbf{c}^T\mathbf{R}_{yy}\mathbf{c}-2\mathbf{c}^T\mathbf{R}_{yx}+\mathbf{R}_{xx}
\end{aligned}$$

where the covariance matrix $\mathbf{R}_{yy}$ is defined as $\mathbf{R}_{yy}=\mathrm{E}\left\{\mathbf{y}\mathbf{y}^H\right\}$. Similarly, $\mathbf{R}_{yx}=\mathrm{E}\left\{\mathbf{y}x\right\}$ $=\mathbf{R}_{xy}^T$ and $\mathbf{R}_{xx}=\mathrm{E}\left\{x^2\right\}$. Also note that we have used the fact $\mathbf{c}^T\mathbf{R}_{yx}=\left(\mathbf{c}^T\mathbf{R}_{yx}\right)^T=$ $\mathbf{R}_{xy}\mathbf{c}$. Hence, the average MSE as a function of the receive beamformer $\mathbf{c}$, denoted by $\overline{\text{MSE}}\left(\mathbf{c}\right)$, is given as

$$\overline{\text{MSE}}\left(\mathbf{c}\right)=\mathbf{c}^T\mathbf{R}_{yy}\mathbf{c}-2\mathbf{c}^T\mathbf{R}_{yx}+\mathbf{R}_{xx}$$

where the covariance matrix $\mathbf{R}_{yy}$ is defined as $\mathbf{R}_{yy}=\mathrm{E}\left\{\mathbf{y}\mathbf{y}^H\right\}$. Similarly, $\mathbf{R}_{yx}=\mathrm{E}\left\{\mathbf{y}x\right\}$ $=\mathbf{R}_{xy}^T$ and $\mathbf{R}_{xx}=\mathrm{E}\left\{x^2\right\}$. Also note that we have used the fact $\mathbf{c}^T\mathbf{R}_{yx}=\left(\mathbf{c}^T\mathbf{R}_{yx}\right)^T=$ $\mathbf{R}_{xy}\mathbf{c}$. Hence, the average MSE as a function of the receive beamformer $\mathbf{c}$, denoted by $\overline{\text{MSE}}\left(\mathbf{c}\right)$, is given as

$$\overline{\text{MSE}}\left(\mathbf{c}\right)=\mathbf{c}^T\mathbf{R}_{yy}\mathbf{c}-2\mathbf{c}^T\mathbf{R}_{yx}+\mathbf{R}_{xx}$$

Thus, the optimal beamformer $\mathbf{c}$ which minimizes the average or mean squared error can be obtained by differentiating $\overline{\text{MSE}}\left(\mathbf{c}\right)$ with respect to $\mathbf{c}$ and setting equal to zero as

$$\begin{aligned}
\frac{\partial\overline{\text{MSE}}\left(\mathbf{c}\right)}{\partial\mathbf{c}} &= 0 \\
\frac{\partial}{\partial\mathbf{c}}\left(\mathbf{c}^T\mathbf{R}_{yy}\mathbf{c}-2\mathbf{c}^T\mathbf{R}_{yx}+\mathbf{R}_{xx}\right) &= 0 \\
2\mathbf{R}_{yy}\mathbf{c}-2\mathbf{R}_{yx} &= 0 \\
\mathbf{c} &= \mathbf{R}_{yy}^{-1}\mathbf{R}_{yx}
\end{aligned}$$

Thus, the optimal LMMSE beamforming vector $\mathbf{c}$ is given as $\mathbf{c}=\mathbf{R}_{yy}^{-1}\mathbf{R}_{yx}$. This is also termed in signal processing as the optimal *Wiener* filter. The above can be generalized in the case of complex vectors by replacing the transpose by the Hermitian operation.

Hence, the MMSE estimate of x is given as

$$\begin{aligned}\hat{\mathbf{x}}_{\text{MMSE}} &= \mathbf{c}^H \mathbf{y} \\ &= \left(\mathbf{R}_{yy}^{-1}\mathbf{R}_{yx}\right)^H \mathbf{y} \\ &= \mathbf{R}_{xy}\mathbf{R}_{yy}^{-1}\mathbf{y}\end{aligned}$$

We now compute the MMSE receiver for the MIMO wireless system. Consider again the MIMO system model given as

$$\mathbf{y} = \mathbf{H}\mathbf{x} + \mathbf{n}$$

Let the transmit symbols x_i, $1 \leq i \leq t$ be such that each is of power P_d, i.e., $\mathrm{E}\left\{|x_i|^2\right\} = P_d$, with elements on different transmit antennas being uncorrelated, i.e., $\mathrm{E}\left\{x_i x_j^*\right\} = 0$ when $i \neq j$. Hence, the covariance $\mathbf{R}_{xx}$ of the transmit symbols is given as

$$
\begin{aligned}
\mathbf{R}_{xx} &= \mathrm{E}\left\{\mathbf{x}\mathbf{x}^H\right\} \\
&= \mathrm{E}\left\{\begin{bmatrix} x_1 \\ x_2 \\ \vdots \\ x_t \end{bmatrix} \begin{bmatrix} x_1^* & x_2^* & \dots & x_t^* \end{bmatrix}\right\} \\
&= \begin{bmatrix} \mathrm{E}\left\{|x_1|^2\right\} & \mathrm{E}\{x_1 x_2^*\} & \dots & \mathrm{E}\{x_1 x_t^*\} \\ \mathrm{E}\{x_2 x_1^*\} & \mathrm{E}\left\{|x_2|^2\right\} & \dots & \mathrm{E}\{x_2 x_t^*\} \\ \vdots & \vdots & \ddots & \vdots \\ \mathrm{E}\{x_t x_1^*\} & \mathrm{E}\{x_t x_2^*\} & \dots & \mathrm{E}\left\{|x_t|^2\right\} \end{bmatrix} \\
&= \begin{bmatrix} P_d & 0 & 0 & \dots & 0 \\ 0 & P_d & 0 & \dots & 0 \\ \vdots & \vdots & \vdots & \ddots & \vdots \\ 0 & 0 & 0 & \dots & P_d \end{bmatrix} \\
&= P_d \mathbf{I}_t
\end{aligned}
$$

Hence, $\mathbf{R}_{yy}$, the covariance of the receive vector $\mathbf{y}$ can be simplified as

$$
\begin{aligned}
\mathbf{R}_{yy} &= \mathrm{E}\left\{\mathbf{y}\mathbf{y}^H\right\} \\
&= \mathrm{E}\left\{(\mathbf{H}\mathbf{x} + \mathbf{n})(\mathbf{H}\mathbf{x} + \mathbf{n})^H\right\} \\
&= \mathrm{E}\left\{\mathbf{H}\mathbf{x}\mathbf{x}^H\mathbf{H} + \mathbf{n}\mathbf{x}^H\mathbf{H}^H + \mathbf{H}\mathbf{x}\mathbf{n}^H + \mathbf{n}\mathbf{n}^H\right\}
\end{aligned}
$$

$$= \mathbf{H}\underbrace{\mathrm{E}\left\{\mathbf{x}\mathbf{x}^H\right\}}_{\mathbf{R}_{xx}}\mathbf{H} + \underbrace{\mathrm{E}\left\{\mathbf{n}\mathbf{x}^H\right\}}_{0}\mathbf{H}^H + \mathbf{H}\underbrace{\mathrm{E}\left\{\mathbf{x}\mathbf{n}^H\right\}}_{0} + \underbrace{\mathrm{E}\left\{\mathbf{n}\mathbf{n}^H\right\}}_{\mathbf{R}_{nn}}$$

$$= \underbrace{P_d\mathbf{H}\mathbf{H}^H + \sigma_n^2\mathbf{I}_r}_{\mathbf{R}_{yy}}$$

where we have used the fact that $\mathrm{E}\left\{\mathbf{n}\mathbf{x}^H\right\} = \mathrm{E}\left\{\mathbf{x}\mathbf{n}^H\right\} = \mathbf{0}$, since the noise at receiver and transmit symbols are uncorrelated, in the above simplification. Further, cross-covariance matrix $\mathbf{R}_{yx}$ can be simplified as

$$\begin{aligned}
\mathbf{R}_{yx} &= \mathrm{E}\left\{\mathbf{y}\mathbf{x}^H\right\} \\
&= \mathrm{E}\left\{\left(\mathbf{H}\mathbf{x} + \mathbf{n}\right)\mathbf{x}^H\right\} \\
&= \mathrm{E}\left\{\mathbf{H}\mathbf{x}\mathbf{x}^H + \mathbf{n}\mathbf{x}^H\right\} \\
&= \mathbf{H}\underbrace{\mathrm{E}\left\{\mathbf{x}\mathbf{x}^H\right\}}_{\mathbf{R}_{xx}} + \underbrace{\mathrm{E}\left\{\mathbf{n}\mathbf{x}^H\right\}}_{0} \\
&= P_d\mathbf{H}
\end{aligned}$$

Thus, the optimal MMSE receiver is given as

$$\begin{aligned}
\mathbf{C} &= \mathbf{R}_{yy}^{-1}\mathbf{R}_{yx} \\
&= \left(P_d\mathbf{H}\mathbf{H}^H + \sigma_n^2\mathbf{I}\right)^{-1}P_d\mathbf{H} \\
&= P_d\left(P_d\mathbf{H}\mathbf{H}^H + \sigma_n^2\mathbf{I}\right)^{-1}\mathbf{H}
\end{aligned}$$

Hence, the MMSE estimate $\hat{\mathbf{x}}_{\text{MMSE}}$ of the transmit vector $\mathbf{x}$ is given as

$$\underline{\hat{\mathbf{x}}_{\text{MMSE}} = \mathbf{C}^H\mathbf{y}}$$

We now derive an alternative structure for the MIMO MMSE receiver. Observe that, we have,

$$P_d\mathbf{H}^H\mathbf{H}\mathbf{H}^H + \sigma_n^2\mathbf{H}^H = P_d\mathbf{H}^H\mathbf{H}\mathbf{H}^H + \sigma_n^2\mathbf{H}^H$$

$$\Rightarrow \left(P_d\mathbf{H}^H\mathbf{H} + \sigma_n^2\mathbf{I}\right)\mathbf{H}^H = \mathbf{H}^H\left(P_d\mathbf{H}\mathbf{H}^H + \sigma_n^2\mathbf{I}\right)$$

$$\Rightarrow \mathbf{H}^H\left(P_d\mathbf{H}\mathbf{H}^H + \sigma_n^2\mathbf{I}\right)^{-1} = \left(P_d\mathbf{H}^H\mathbf{H} + \sigma_n^2\mathbf{I}\right)^{-1}\mathbf{H}^H$$

Thus, the MIMO MMSE receiver in Eq. (6.8) can also be expressed as

$$\begin{aligned}\hat{\mathbf{x}}_{\text{MMSE}} &= P_d \mathbf{H}^H \left(P_d \mathbf{H}\mathbf{H}^H + \sigma_n^2 \mathbf{I}\right)^{-1} \mathbf{y} \\ &= P_d \left(P_d \mathbf{H}^H \mathbf{H} + \sigma_n^2 \mathbf{I}\right)^{-1} \mathbf{H}^H \mathbf{y} \end{aligned} \tag{6.9}$$

Thus, the above expression is an alternative form of implementation of the MIMO MMSE receiver. Observe that the matrix $\mathbf{H}\mathbf{H}^H + \sigma_n^2 \mathbf{I}$ is of dimension $r \times r$, while $P_d \mathbf{H}^H \mathbf{H} + \sigma_n^2 \mathbf{I}$ is $t \times t$ dimensional. Thus, if $r > t$, inversion of the latter matrix is of a lower computation complexity. Since this is frequently the case in MIMO wireless systems, the alternative MIMO MMSE receiver version is more popular for implementation.

Qn 9 a

LTE was designed with the following objectives in mind to effectively meet the growing demand [13].

- **Performance on Par with Wired Broadband**: One of the goals of LTE was to make mobile Internet experience as good as or better than that achieved by residential wired broadband access systems deployed today. The two key network performance parameters that drive user experience are high throughput and low latency.

  To push toward high throughputs, 3GPP set the peak data rate targets to be at 100Mbps and 50Mbps for the downlink and uplink, respectively. This is an order of magnitude better than what is achieved by 3G systems today. In addition to peak data rates, which may be experienced only by a fraction of users who happen to be in close radio proximity to the base stations, an average user data rate target was also set. The LTE design goal was to achieve an average downlink throughput that is 3–4 times better than that of the original HSPA and an average uplink throughput that is 2–3 times better. It was also stipulated that these higher data rates be achieved by making a 2–4 times improvement in spectral efficiency. LTE requirements also call for increased cell edge bit rate while maintaining the same site locations as deployed today.

  To enable support for delay sensitive applications like voice and interactive gaming, it is required that the network latency is kept very low. The target round-trip latency for LTE radio network is set to be less than 10ms. This is better than the 20–40ms delay observed in many DSL systems. In addition, LTE aims to reduce latency associated with control plane functions such as session setup. Enhancing QoS capabilities to support a variety of applications is another LTE goal.

  While LTE aims for performance parity with wired broadband systems, it does so while simultaneously elevating the requirements on mobility. The system is required to support optimized high quality handoff and connections up to speeds of 15kmph with only minor degradations allowed for connections up to speeds of 120kmph. A lower quality support is envisioned for up to 350kmph.

- **Flexible Spectrum Usage**: The frequency band and amount of spectrum owned by different mobile operators around the world vary significantly. Since many LTE deployments are likely to be in refarmed spectrum that is currently used for 3G or 2G services, the amount of spectrum that could be made available for LTE will also depend on how aggressively individual operators wish to migrate to LTE. In order to be a truly global standard and to make it attractive for deployment by a wide variety of operators, 3GPP mandated a high degree of spectrum flexibility.
- **Co-existence and Interworking with 3G Systems as well as Non-3GPP Systems**: Given the large base of existing mobile subscribers, it is a critical requirement that LTE networks interwork seamlessly with existing 2G and 3G systems. Most existing cellular operators are likely to phase in LTE over a period of time with initial deployments being made in areas of high demand such as urban cores. Service continuity and mobility—handoff and roaming—between LTE and existing 2G/3G systems are critical to obtain a seamless user experience. As LTE aims to be a truly global standard attractive to a variety of operators, interworking requirements have been extended to non-3GPP systems such as the 3GPP2 CDMA and WiMAX networks. Further, to facilitate fixed-mobile convergence, interworking requirements apply to all IP networks including wired IP networks
- **Reducing Cost per Megabyte**: As discussed in the previous section, there is a growing gap between wireless data consumption and revenue. To bridge this gap, it is essential that substantial reductions be achieved in the total network cost to deliver data to end users. 3GPP recognizes this issue and has made reducing the cost per megabyte of data a key design criterion for LTE. A number of design criteria are tied directly to cost efficiency. These include:

  - High-capacity, high-spectral efficiency air-interface
  - Ability to deploy in existing spectrum and reuse cell sites and transmission equipment
  - Interworking with legacy systems to allow for cost-effective migration
  - Interworking with non-3GPP systems to drive toward one global standard to achieve higher economies of scale
  - A flat architecture with fewer network components and protocols
  - A single IP packet core for voice and data

Qn 9 b

To efficiently support various QoS classes of services, LTE adopts a hierarchical channel structure. There are three different channel types defined in LTE—logical channels, transport channels, and physical channels, each associated with a service access point (SAP) between different layers. These channels are used by the lower layers of the protocol stack to provide services to the higher layers. The radio interface protocol architecture and the SAPs between different layers are shown in Figure 6.5. Logical channels provide services at the SAP between MAC and RLC layers, while transport channels provide services at the SAP between MAC and PHY layers. Physical channels are the actual implementation of transport channels over the radio interface.

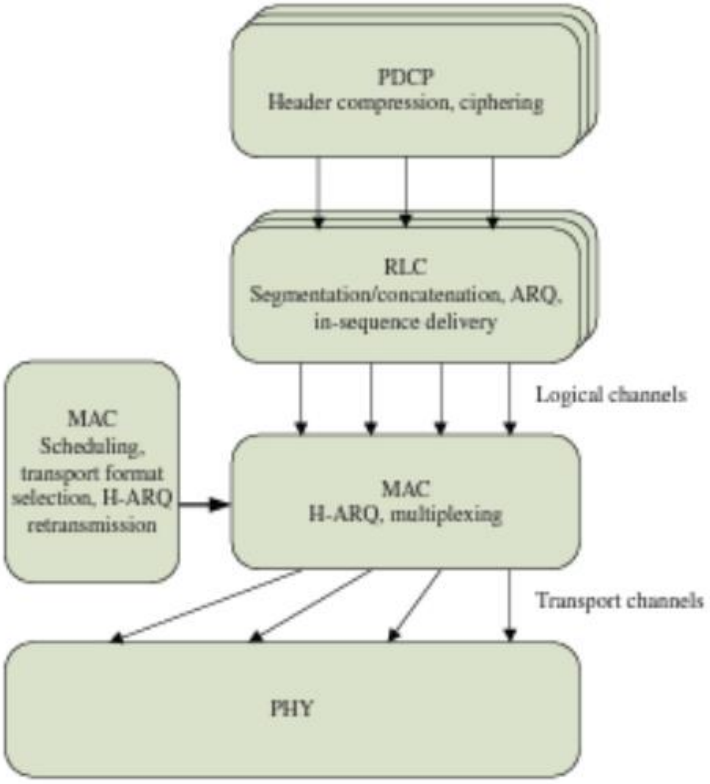

Figure 6.5 The radio interface protocol architecture and the SAPs between different layers.

The channels defined in LTE follow a similar hierarchical structure to UTRA/HSPA. However, in the case of LTE, the transport and logical channel structures are much more simplified and fewer in number compared to UTRA/HSPA. Unlike UTRA/HSPA, LTE is based entirely on shared and broadcast channels and contains no dedicated channels carrying data to specific UEs. This improves the efficiency of the radio interface and can support dynamic resource allocation between different UEs depending on their traffic/QoS requirements and their respective channel conditions. In this section, we describe in detail the various logical, transport, and physical channels that are defined in LTE.

The logical control channels, which are used to transfer control plane information, include the following types:

- **Broadcast Control Channel (BCCH):** A downlink common channel used to broadcast system control information to the mobile terminals in the cell, including downlink system bandwidth, antenna configuration, and reference signal power. Due to the large amount of information carried on the BCCH, it is mapped to two different transport channels: the Broadcast Channel (BCH) and the Downlink Shared Channel (DL-SCH).

- **Multicast Control Channel (MCCH):** A point-to-multipoint downlink channel used for transmitting control information to UEs in the cell. It is only used by UEs that receive multicast/broadcast services.

- **Paging Control Channel (PCCH):** A downlink channel that transfers paging information to registered UEs in the cell, for example, in case of a mobile-terminated communication session. The paging process is discussed in Chapter 10.

- **Common Control Channel (CCCH):** A bi-directional channel for transmitting control information between the network and UEs when no RRC connection is available, implying the UE is not attached to the network such as in the idle state. Most commonly the CCCH is used during the random access procedure.

- **Dedicated Control Channel (DCCH):** A point-to-point, bi-directional channel that transmits dedicated control information between a UE and the network. This channel is used when the RRC connection is available, that is, the UE is attached to the network.

The logical traffic channels, which are to transfer user plane information, include:

- **Dedicated Traffic Channel (DTCH):** A point-to-point, bi-directional channel used between a given UE and the network. It can exist in both uplink and downlink.
- **Multicast Traffic Channel (MTCH):** A unidirectional, point-to-multipoint data channel that transmits traffic data from the network to UEs. It is associated with the multicast/broadcast service.

Qn 10 a

In LTE specifications, the size of elements in the time domain is expressed as a number of time units $T_s = 1/(15000 \times 2048)$ seconds. As the normal subcarrier spacing is defined to be $\Delta f = 15$kHz, T_s can be regarded as the sampling time of an FFT-based OFDM transmitter/receiver implementation with FFT size $N_{\text{FFT}} = 2048$. Note that this is just for notation purpose, as different FFT sizes are supported depending on the transmission bandwidths. A set of parameters for typical transmission bandwidths for LTE in the downlink is shown in Table 6.2, where the subcarrier spacing is $\Delta f = 15$kHz. The FFT size increases with the transmission bandwidth, ranging from 128 to 2048. With $\Delta f = 15$kHz, the sampling frequency, which equals $\Delta f \times N_{\text{FFT}}$, is a multiple or sub-multiple of the UTRA/HSPA chip rate of 3.84MHz. In this way, multimode UTRA/HSPA/LTE terminals can be implemented with a single clock circuitry. In addition to the 15kHz subcarrier spacing, a *reduced subcarrier spacing* of 7.5kHz is defined for MBSFN cells, which provides a larger OFDM symbol duration that is able to combat the large delay spread associated with the MBSFN transmission. Unless otherwise stated, we will assume $\Delta f = 15$kHz in the following discussion.

In the time domain, the downlink and uplink multiple TTIs are organized into radio frames with duration $T_f = 307200 \cdot T_s = 10$ ms. For flexibility, LTE supports both FDD and TDD modes.[5] Most of the design parameters are common to FDD and TDD in order to reduce the terminal complexity and maximize reuse between the designs of FDD and TDD systems. Accordingly, LTE supports two kinds of frame structures: frame structure type 1 for the FDD mode and frame structure type 2 for the TDD mode.

Frame Structure Type 1

Frame structure type 1 is applicable to both full duplex and half duplex FDD. There are three different kinds of units specified for this frame structure, illustrated in Figure 6.8. The smallest one is called a *slot*, which is of length $T_{slot} = 15360 \cdot T_s = 0.5$ ms. Two consecutive slots are defined as a *subframe* of length 1 ms, and 20 slots, numbered from 0 to 19, constitute a *radio frame* of 10 ms. Channel-dependent scheduling and link adaptation operate on a subframe level. Therefore, the subframe duration corresponds to the minimum downlink TTI, which is of 1 ms duration, compared to a 2 ms TTI for the HSPA and a minimum 10 ms TTI for the UMTS. A shorter TTI is for fast link adaptation and is able to reduce delay and better exploit the time-varying channel through channel-dependent scheduling.

Table 6.2 Typical Parameters for Downlink Transmission

Transmission bandwidth [MHz]	1.4	3	5	10	15	20
Occupied bandwidth [MHz]	1.08	2.7	4.5	9.0	13.5	18.0
Guardband [MHz]	0.32	0.3	0.5	1.0	1.5	2.0
Guardband, % of total	23	10	10	10	10	10
Sampling frequency [MHz]	1.92 $1/2 \times 3.84$	3.84	7.68 2×3.84	15.36 4×3.84	23.04 6×3.84	30.72 8×3.84
FFT size	128	256	512	1024	1536	2048
Number of occupied subcarriers	72	180	300	600	900	1200
Number of resource blocks	6	15	25	50	75	100
Number of CP samples (normal)	9×6 10×1	18×6 20×1	36×6 40×1	72×6 80×1	108×6 120×1	144×6 160×1
Number of CP samples (extended)	32	64	128	256	384	512

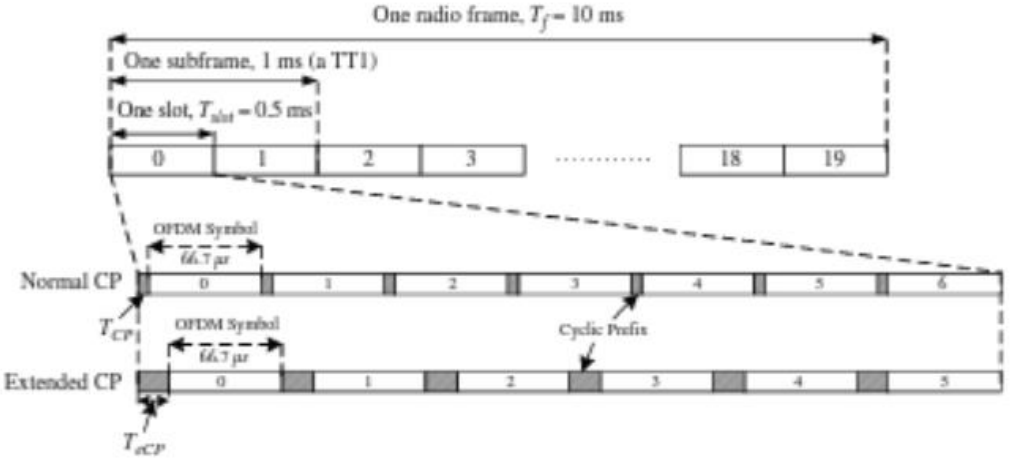

Figure 6.8 Frame structure type 1. For the normal CP, $T_{CP} = 160 \cdot T_s \approx 5.2\mu s$ for the first OFDM symbol, and $T_{CP} = 144 \cdot T_s \approx 4.7\mu s$ for the remaining OFDM symbols, which together fill the entire slot of 0.5 ms. For the extended CP, $T_{eCP} = 512 \cdot T_s \approx 16.7\mu s$.

Frame Structure Type 2

Frame structure type 2 is applicable to the TDD mode. It is designed for coexistence with legacy systems such as the 3GPP TD-SCDMA-based standard. As shown in Figure 6.9, each radio frame of frame structure type 2 is of length $T_f = 30720 \cdot T_s = 10$ ms, which

consists of two half-frames of length 5 ms each. Each half-frame is divided into five subframes with 1 ms duration. There are special subframes, which consist of three fields: Downlink Pilot TimeSlot (DwPTS), Guard Period (GP), and Uplink Pilot TimeSlot (UpPTS). These fields are already defined in TD-SCDMA and are maintained in the LTE TDD mode to provide sufficiently large guard periods for the equipment to switch between transmission and reception.

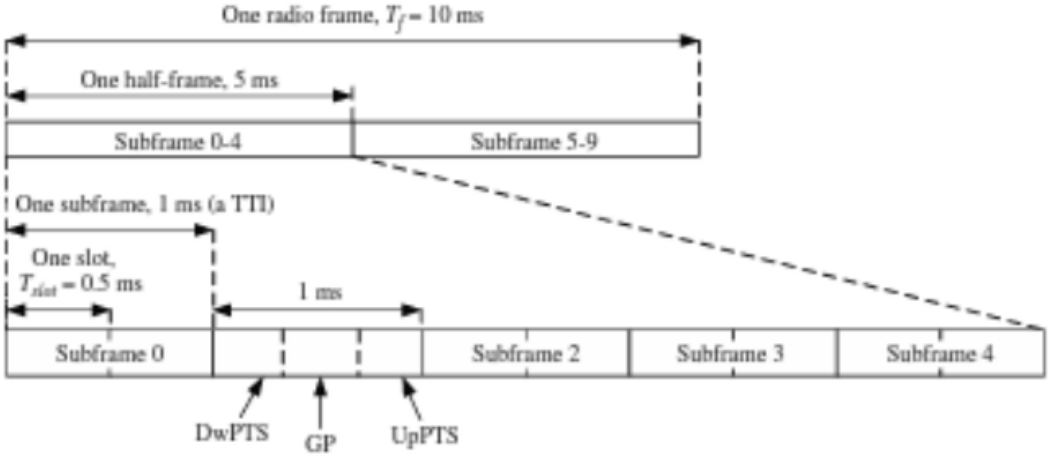

Figure 6.9 Frame structure type 2.

- **The DwPTS field:** This is the downlink part of the special subframe, and can be regarded as an ordinary but shorter downlink subframe for downlink data transmission. Its length can be varied from three up to twelve OFDM symbols.
- **The UpPTS field:** This is the uplink part of the special subframe, and has a short duration with one or two OFDM symbols. It can be used for transmission of uplink sounding reference signals and random access preambles.
- **The GP field:** The remaining symbols in the special subframe that have not been allocated to DwPTS or UpPTS are allocated to the GP field, which is used to provide the guard period for the downlink-to-uplink and the uplink-to-downlink switch.

Qn 10 b

For the LTE uplink transmission, SC-FDMA with a CP is adopted. As discussed in Chapter 4, SC-FDMA possesses most of the merits of OFDM while enjoying a lower PAPR. A lower PAPR is highly desirable in the uplink as less expensive power amplifiers are needed at UEs and the coverage is improved. In LTE, the SC-FDMA signal is generated by the DFT-spread-OFDM. Compared to conventional OFDM, the SC-FDMA receiver has higher complexity, which, however, is not considered to be an issue in the uplink given the powerful computational capability at the base station.

An SC-FDMA transceiver has a similar structure as OFDM, so the parametrization of radio resource in the uplink enjoys similarities to that in the downlink described in Section 6.3. Nevertheless, the uplink transmission has its own properties. Different from the downlink, only localized resource allocation on consecutive subcarriers is allowed in the uplink. In addition, only limited MIMO modes are supported in the uplink. In this section, we focus on the differences in the uplink radio resource from that in the downlink.

6.4.1 Frame Structure

The uplink frame structure is similar to that for the downlink. The difference is that now we talk about *SC-FDMA symbols* and *SC-FDMA subcarriers*. In frame structure type 1, an uplink radio frame consists of 20 slots of 0.5 ms each, and one subframe consists of two slots, as in Figure 6.8. Frame structure type 2 consists of ten subframes, with one or two special subframes including DwPTS, GP, and UpPTS fields, as shown in Figure 6.9. A CP is inserted prior to each SC-FDMA symbol. Each slot carries seven SC-FDMA symbols in the case of normal CP, and six SC-FDMA symbols in the case of extended CP.

6.4.2 Physical Resource Blocks for SC-FDMA

As SC-FDMA can be regarded as conventional OFDM with a DFT-based precoder, the *resource grid* for the uplink is similar to the one for the downlink, illustrated in Figure 6.12, that is, it comprises a number of resource blocks in the time-frequency plane. The number of resource blocks in each resource grid, N_{RB}^{UL}, depends on the uplink transmission bandwidth configured in the cell and should satisfy

$$N_{RB}^{min,UL} \leq N_{RB}^{UL} \leq N_{RB}^{max,UL},$$

where $N_{RB}^{min,UL} = 6$ and $N_{RB}^{max,UL} = 110$ correspond to the smallest and largest uplink bandwidth, respectively. There are $N_{sc}^{RB} \times N_{symb}^{RB}$ resource elements in each resource block. The values of N_{sc}^{RB} and N_{symb}^{UL} for normal and extended CP are given in Table 6.6. There is only one subcarrier spacing supported in the uplink, which is $\Delta f = 15$kHz. Different from the downlink, the DC subcarrier is used in the uplink, as the DC interference is spread over the modulation symbols due to the DFT-based precoding.

As for the downlink, each *resource element* in the resource grid is uniquely defined by the index pair (k, l) in a slot, where $k = 0, \ldots, N_{RB}^{UL} N_{sc}^{RB} - 1$ and $l = 0, \ldots, N_{symb}^{UL} - 1$ are the indices in the frequency and time domain, respectively. For the uplink, no antenna port is defined, as only single antenna transmission is supported in the current specifications.

Table 6.6 Physical Resource Block Parameters for Uplink

Configuration	N_{sc}^{RB}	N_{symb}^{UL}
Normal CP	12	7
Extended CP	12	6

PRB number n_{PRB} in the frequency domain and resource elements (k, l) in a slot is given by:

$$n_{PRB} = \left\lfloor \frac{k}{N_{sc}^{RB}} \right\rfloor.$$

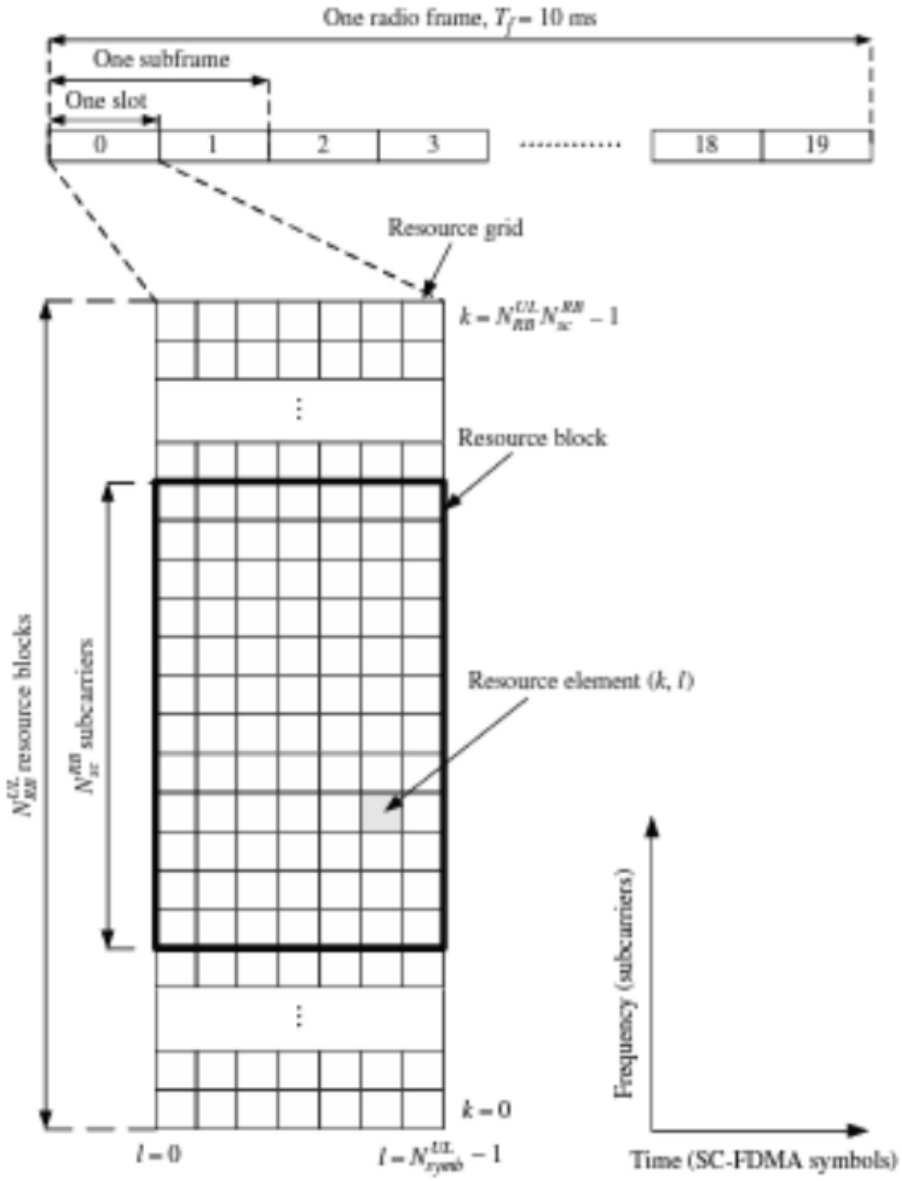

Figure 6.12 The structure of the uplink resource grid.